Lepton-nucleus scattering within the quantum Monte Carlo based approaches

Noemi Rocco

Neutrino Scattering at Low and Intermediate Energies —MITP
Jun 26–30, 2023

Neutrino-nucleus cross section systematics

Current oscillation experiments report **large systematic uncertainties** associated with neutrino-nucleus interaction models.

Error source	ν_e FHC	$\bar{\nu}_e$ RHC	$\nu_e/\bar{\nu}_e$ FHC/RHC
Flux and (ND unconstrained)	15.1	12.2	1.2
cross section (ND constrained)	3.2	3.1	2.7
SK detector	2.8	3.8	1.5
SK FSI + SI + PN	3.0	2.3	1.6
Nucleon removal energy	7.1	3.7	3.6
$\sigma(\nu_e)/\sigma(\bar{\nu}_e)$	2.6	1.5	3.0
NC1γ	1.1	2.6	1.5
NC other	0.2	0.3	0.2
$\sin^2\theta_{23}$ and Δm^2_{21}	0.5	0.3	2.0
$\sin^2\theta_{13}$ PDG2018	2.6	2.4	1.1
All systematics	8.8	7.1	6.0

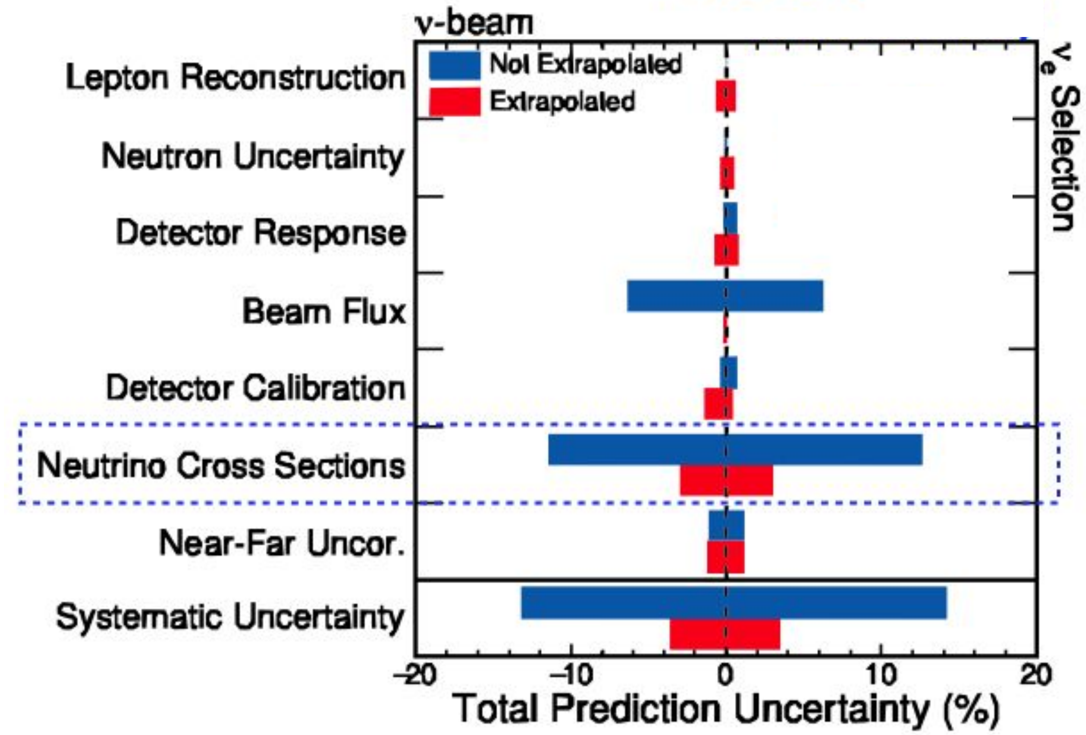

T2K, Phys. Rev. D 103, 112008 (2021)

Noemi Rocco, nrocco@fnal.gov

Hamiltonian and Currents

At low energy, the effective degrees of freedom are pions and nucleons:

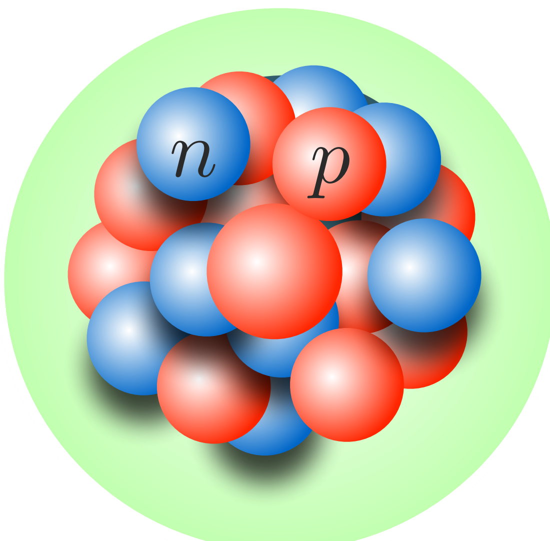

$$H = \sum_i \frac{\mathbf{p}_i^2}{2m} + \sum_{i<j} v_{ij} + \sum_{i<j<k} V_{ijk} + \ldots$$

1-body **2-body** **3-body**

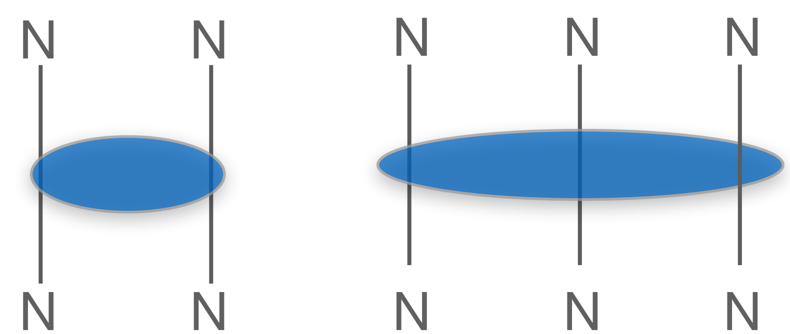

- AV18+IL7
- local chiral interactions (Piarulli et al)

The electromagnetic current is constrained by the Hamiltonian through the **continuity equation**

$$\nabla \cdot \mathbf{J}_{\rm EM} + i[H, J^0_{\rm EM}] = 0 \qquad [v_{ij}, j_i^0] \neq 0$$

The above equation implies that the current operator includes one and two-body contributions

$$J^\mu(q) = \sum_i j_i^\mu + \sum_{i<j} j_{ij}^\mu + \ldots$$

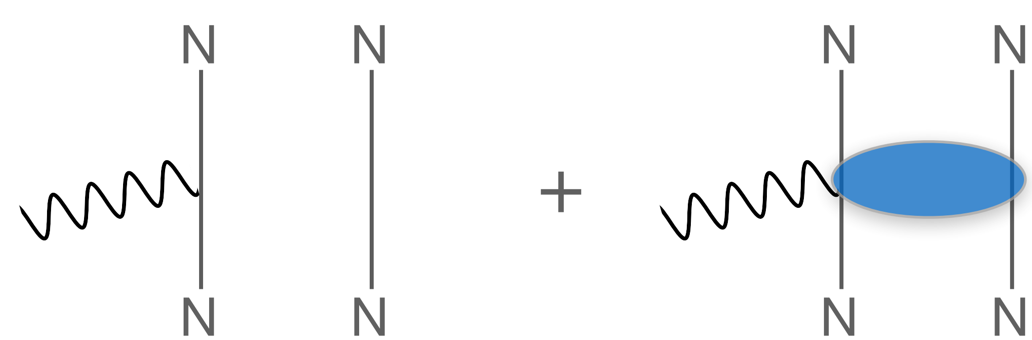

Noemi Rocco, nrocco@fnal.gov

Variational Monte Carlo

In variational Monte Carlo, one **assumes a suitable form for the trial wave function**

$$|\Psi_T\rangle = \mathcal{F}|\Phi\rangle \begin{cases} \Phi : \text{Mean field component; slater determinant of single-particle orbitals} \\ \mathcal{F} : \text{correlations (2b \& 3b) induced by } H \end{cases}$$

The correlation operator reflects the spin-isospin dependence of the nuclear interaction

$$\mathcal{F} \equiv \left(\mathcal{S} \prod_{i<j} F_{ij} \right) \qquad F_{ij} \equiv \sum_p f_{ij}^p O_{ij}^p$$

The best parameters are found by **optimizing the variational energy** $\dfrac{\langle \Psi_T | H | \Psi_T \rangle}{\langle \Psi_T | \Psi_T \rangle} = E_T \geq E_0$

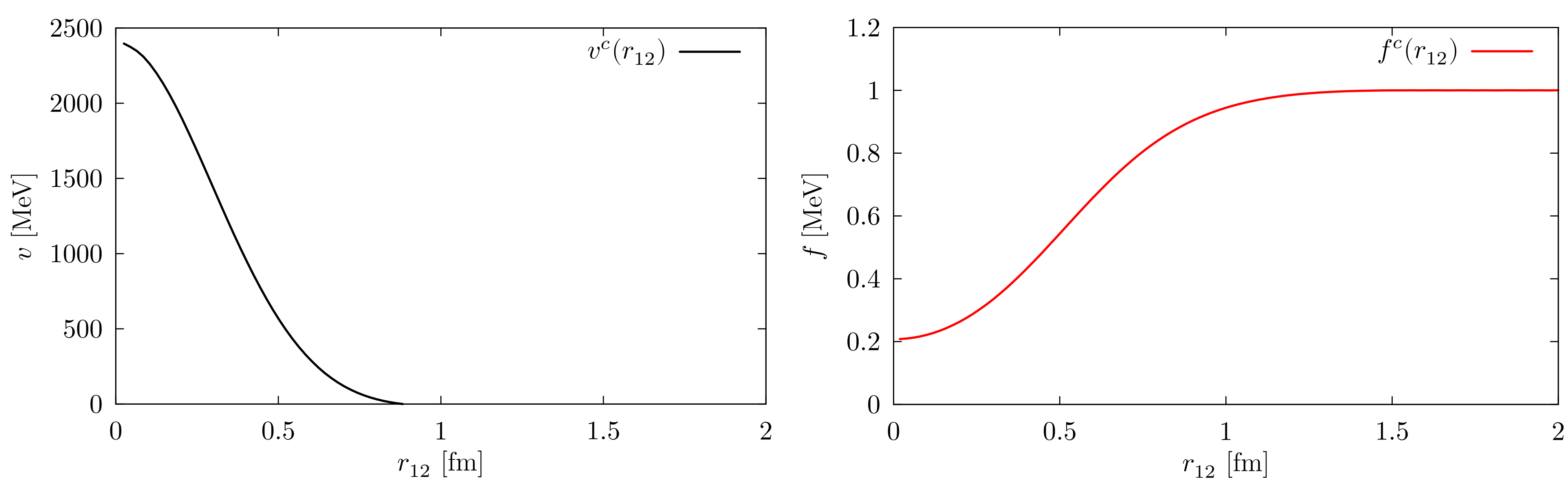

Noemi Rocco, nrocco@fnal.gov
Fermilab

Green's Function Monte Carlo

Any trial wave function can be expanded in the complete set of eigenstates of the the Hamiltonian according to

$$|\Psi_T\rangle = \sum_n c_n |\Psi_n\rangle \qquad H|\Psi_n\rangle = E_n|\Psi_n\rangle$$

GFMC overcomes the limitations of the variational wave-function by using an imaginary-time projection technique to **projects out the exact lowest-energy state**

$$\lim_{\tau\to\infty} e^{-(H-E_0)\tau}|\Psi_T\rangle = \lim_{\tau\to\infty}\sum_n c_n\, e^{-(E_n-E_0)\tau}|\Psi_n\rangle = c_0|\Psi_0\rangle$$

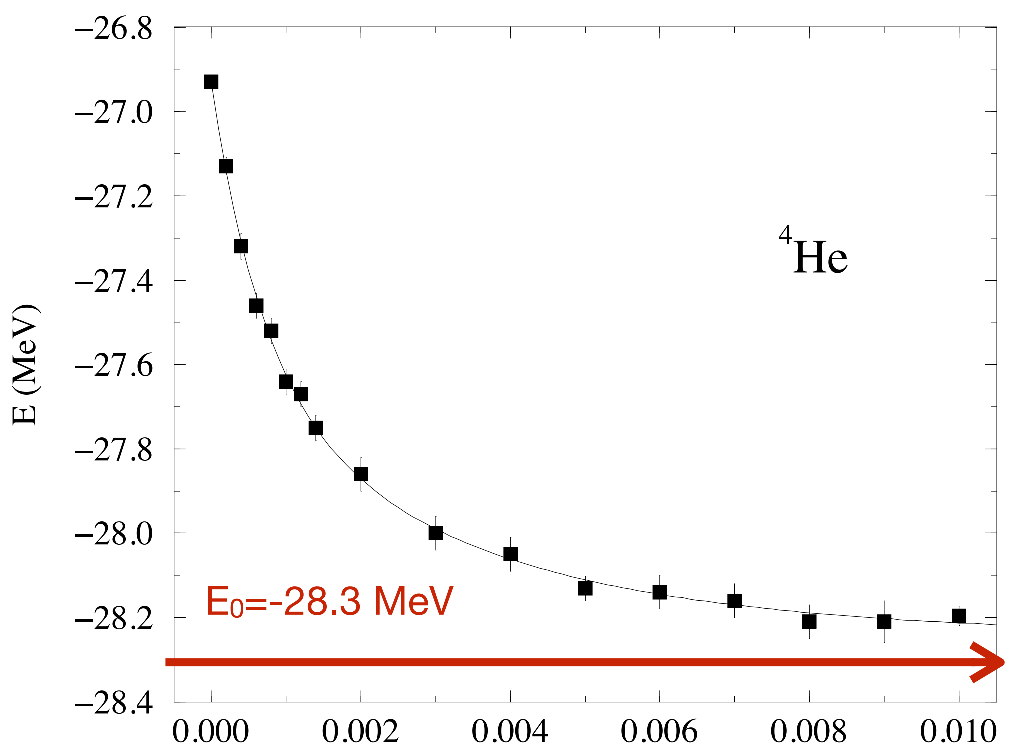

B. Pudliner et al., PRC **56**, 1720 (1997)

The computational cost of the calculation is
2^A x A!/(Z!(A-Z)!)

$$|S\rangle = \begin{pmatrix} s_{\uparrow\uparrow\uparrow} \\ s_{\uparrow\uparrow\downarrow} \\ s_{\uparrow\downarrow\uparrow} \\ s_{\uparrow\downarrow\downarrow} \\ s_{\downarrow\uparrow\uparrow} \\ s_{\downarrow\uparrow\downarrow} \\ s_{\downarrow\downarrow\uparrow} \\ s_{\downarrow\downarrow\downarrow} \end{pmatrix}$$

Noemi Rocco, nrocco@fnal.gov

Green's Function Monte Carlo

Nuclear response function involves evaluating a number of transition amplitudes.
Valuable information can be obtained from the **integral transform of the response function**

$$E_{\alpha\beta}(\sigma,\mathbf{q}) = \int d\omega K(\sigma,\omega) R_{\alpha\beta}(\omega,\mathbf{q}) = \langle\psi_0|J_\alpha^\dagger(\mathbf{q}) K(\sigma, H-E_0) J_\beta(\mathbf{q})|\psi_0\rangle$$

Inverting the integral transform is a complicated problem

A. Lovato et al, PRL117 (2016), 082501, PRC97 (2018), 022502

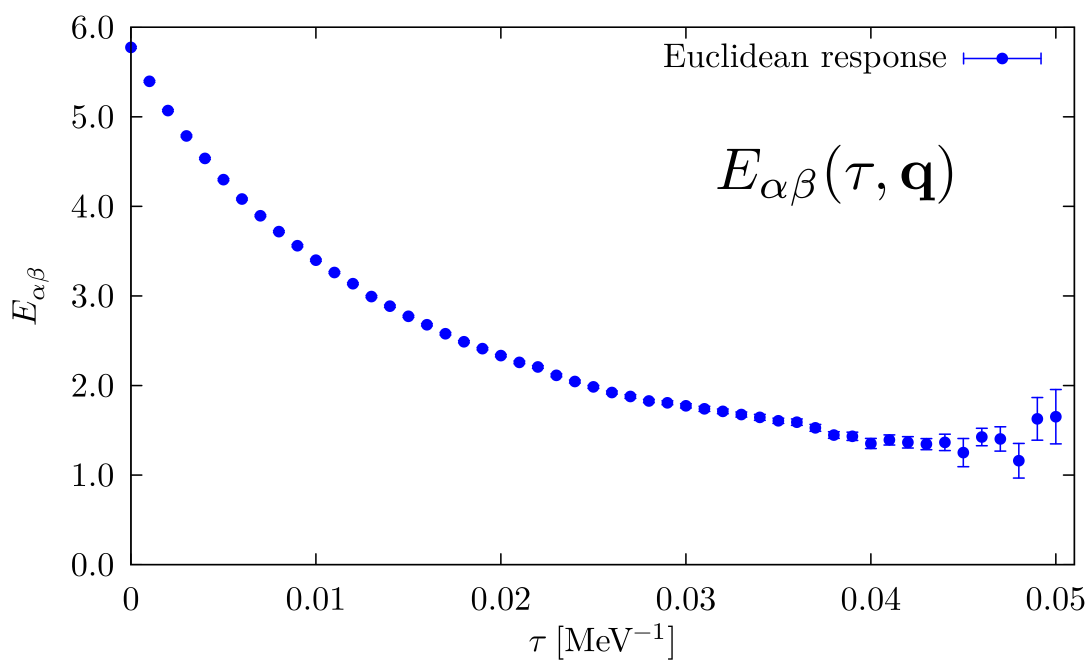

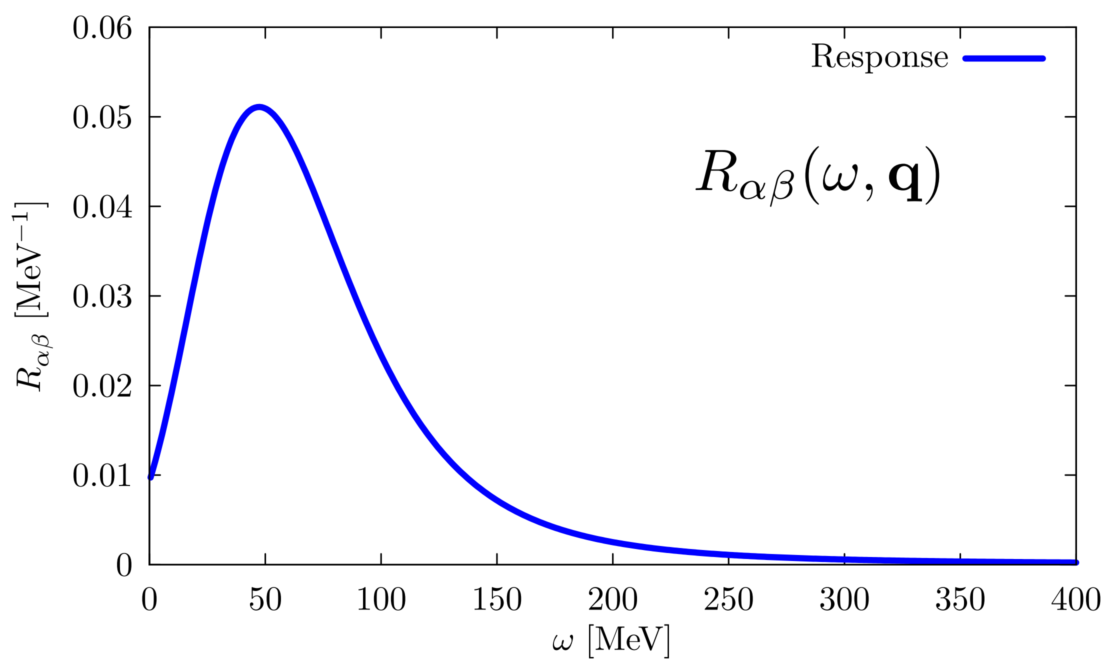

Same problem applies to different realm physics for example lattice QCD

Noemi Rocco, nrocco@fnal.gov

Cross sections: Green's Function Monte Carlo

GFMC accurately obtain the properties of nuclei to ^{12}C using high performance computing

Exact results for ν-cross sections in the **quasi-elastic region** up to moderate values of **q**.

A. Lovato, NR et al , PRX. 10 (2020) 3, 031068

—electron-^{4}He scattering

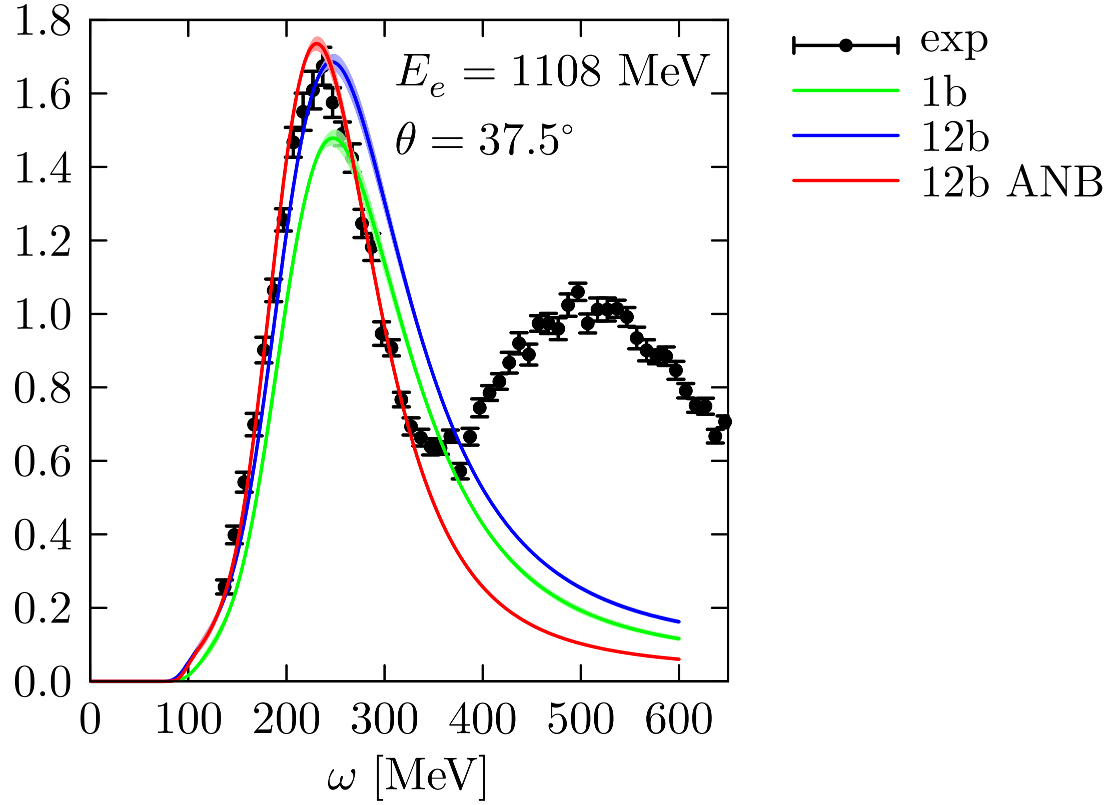

—CC neutrino-^{12}C scattering

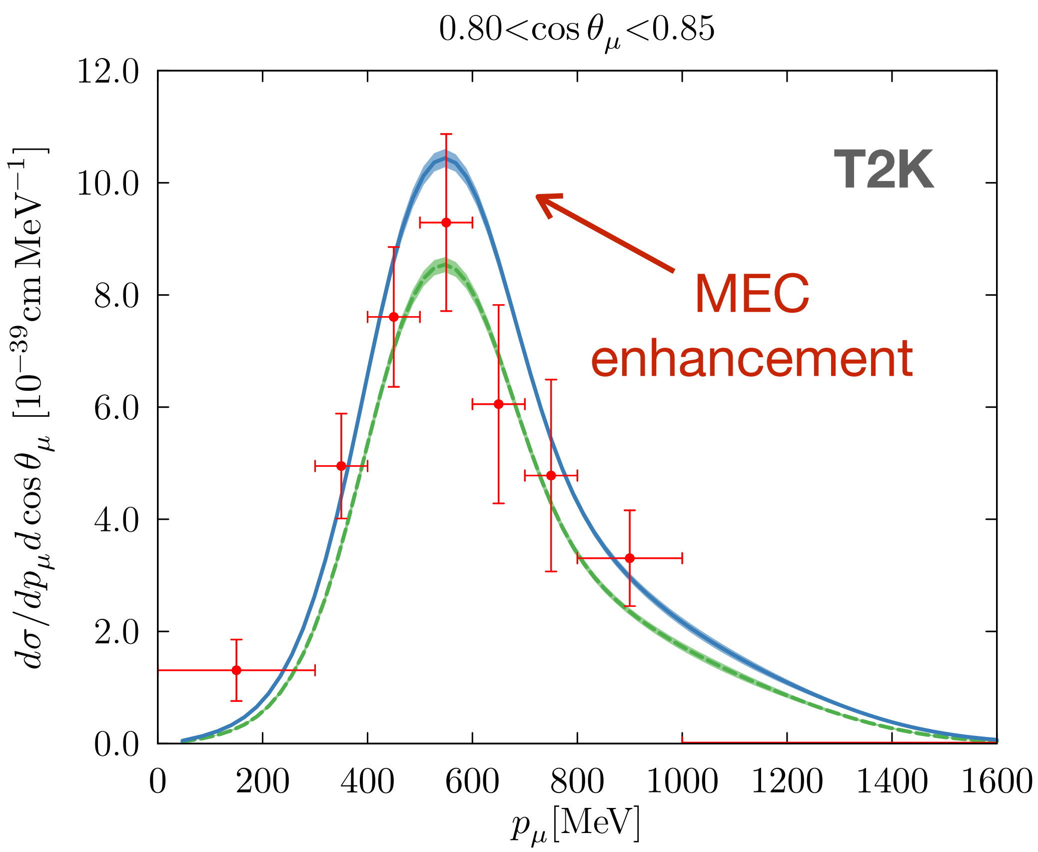

Relies on non-relativistic approximation, inclusive reactions & no explicit pions

Why relativity is important

$$R_{\alpha\beta}(\omega,\mathbf{q}) = \sum_f \underbrace{\langle 0|J^\dagger_\alpha(\mathbf{q})|f\rangle\langle f|J_\beta(\mathbf{q})|0\rangle}_{\text{Currents}}\,\delta(\omega - E_f + E_0) \rightarrow \text{Kinematics}$$

Covariant expression of the e.m. current:

$$j^\mu_{\gamma,S} = \bar{u}(\mathbf{p}')\Big[\frac{G^S_E + \tau G^S_M}{2(1+\tau)}\gamma^\mu + i\frac{\sigma^{\mu\nu}q_\nu}{4m_N}\frac{G^S_M - G^S_E}{1+\tau}\Big]u(\mathbf{p})$$

Nonrelativistic expansion in powers of $\boldsymbol{p}/m_N$

$$j^0_{\gamma,S} = \frac{G^S_E}{2\sqrt{1+Q^2/4m_N^2}} - i\frac{2G^S_M - G^S_E}{8m_N^2}\mathbf{q}\cdot(\boldsymbol{\sigma}\times\mathbf{p})$$

Energy transfer at the quasi-elastic peak:

$$w_{QE} = \sqrt{\mathbf{q}^2 + m_N^2} - m_N \qquad w^{nr}_{QE} = \mathbf{q}^2/(2m_N)$$

Noemi Rocco, nrocco@fnal.gov

Frame dependence

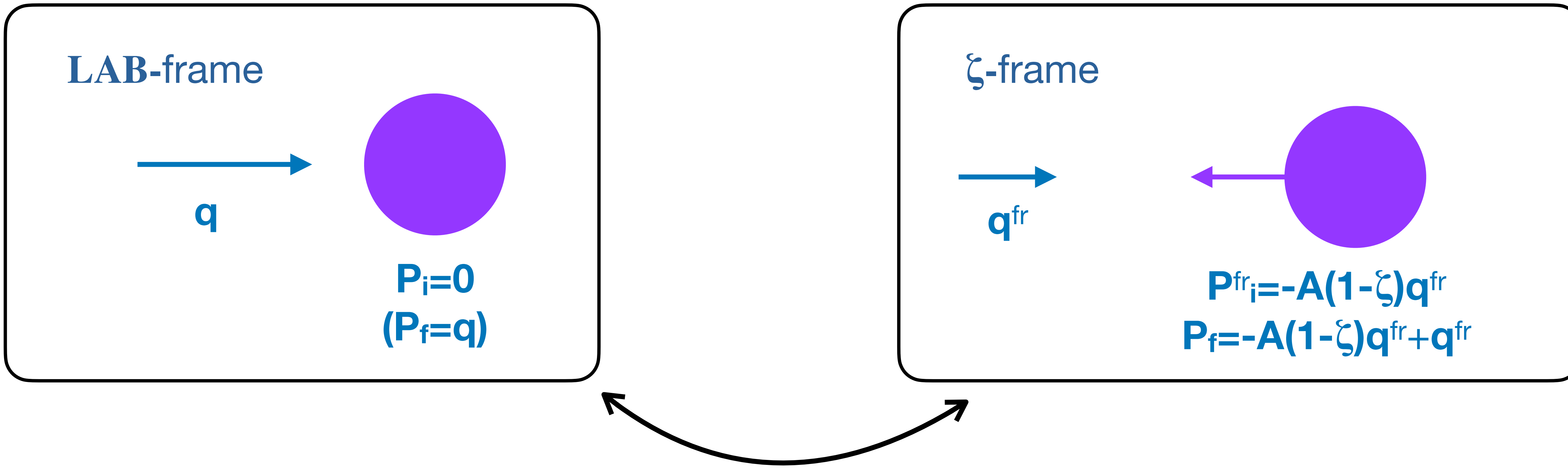

Lorentz Boost connects the two frames

$$R^{\mu\nu}_{LAB}(\omega, q) = B^{\mu}{}_{\alpha}\,[\beta]\,B^{\nu}{}_{\beta}\,[\beta]\,R^{\alpha\beta}_{fr}(\omega^{fr}, \mathbf{q}^{fr})$$

The momentum and energy transfer in the different reference frames are connected:

$$\mathbf{q}^{fr} = \gamma(\mathbf{q} - \boldsymbol{\beta}\omega), \qquad \omega^{fr} = \gamma(\omega - \beta q),$$

Frame dependence

Frame that minimizes relativistic corrections

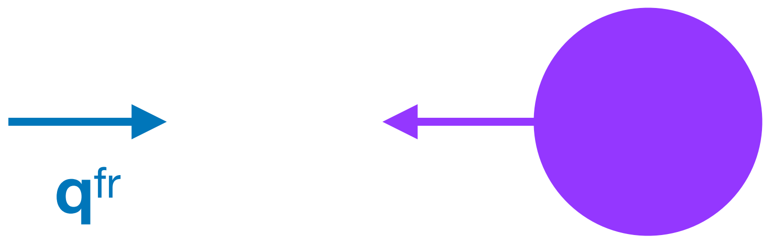

$$\mathbf{P}^{fr}_i = -A/2\ \mathbf{q}^{fr}$$
$$\mathbf{P}_f = -A/2\ \mathbf{q}^{fr} + \mathbf{q}^{fr}$$

- Charge Current electroweak responses of ^{12}C:

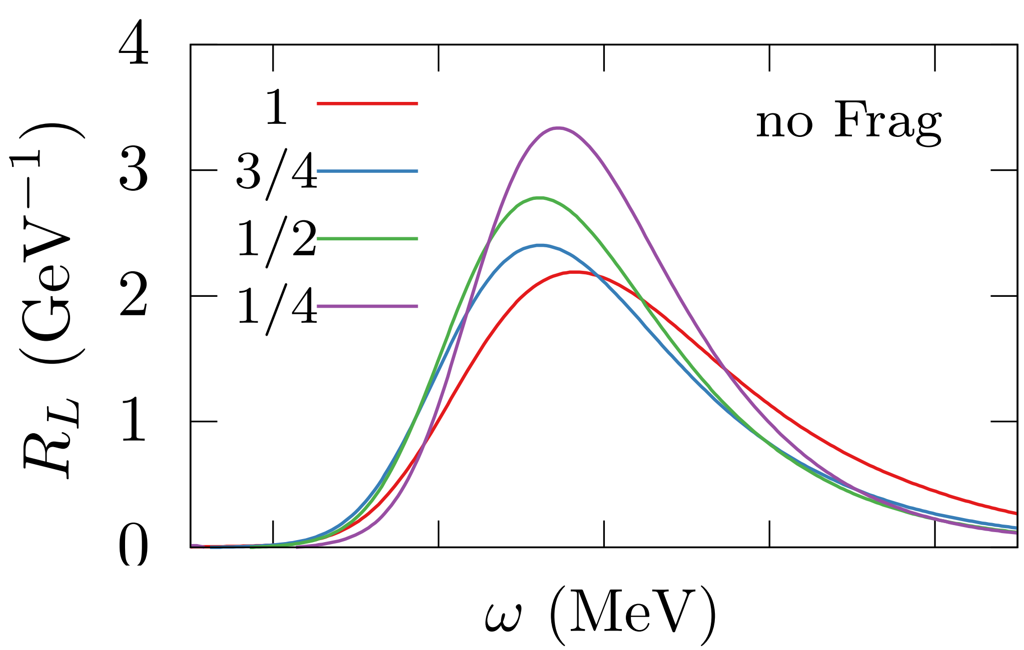

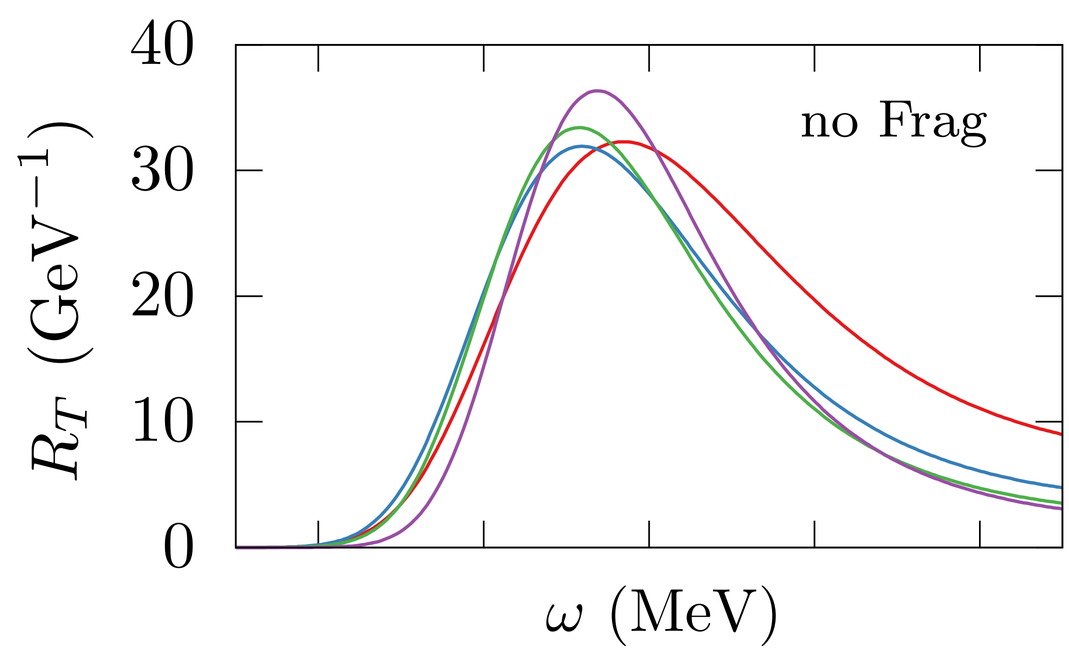

ζ=1/2 Active nucleon Breit frame

- At the single nucleon level:

$$\mathbf{p}^{fr}_i \simeq -\mathbf{q}^{fr}/2$$
$$\mathbf{p}^{fr}_f \simeq \mathbf{q}^{fr}/2$$

- Same position of the quasielastic peak

$$\omega_{QE} = \omega^{nr}_{QE} = 0$$

- Residual frame dependence when boosting back to the LAB-frame

Noemi Rocco, nrocco@fnal.gov

Relativistic effects in a correlated system

Two fragment model:

- The frame dependence can be drastically reduced if one assumes a **two-body breakup model** with **relativistic kinematics** to **determine the input to the non relativistic dynamics calculation**

$$p^{fr} = \mu\Big(\frac{p_N^{fr}}{m_N} - \frac{p_X^{fr}}{M_X}\Big)$$
$$P_f^{fr} = p_N^{fr} + p_X^{fr}$$

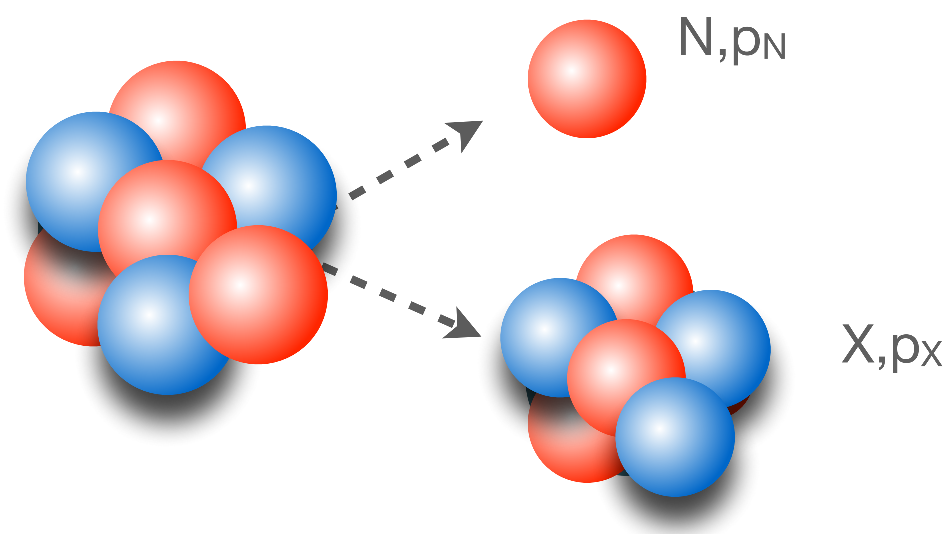

- The relative momentum is derived in a relativistic fashion

$$E_f^{fr} = \sqrt{m_N^2 + [\mathbf{p}^{fr} + \mu/M_X \mathbf{P}_f^{fr}]^2} + \sqrt{M_X^2 + [\mathbf{p}^{fr} - \mu/m_N \mathbf{P}_f^{fr}]^2}$$

$$\omega^{fr} = E_f^{fr} - E_i^{fr}$$

- And it is used as input in the non relativistic kinetic energy

$$e_f^{fr} = (p^{fr})^2/(2\mu)$$

Noemi Rocco, nrocco@fnal.gov
Fermilab

Relativistic effects in a correlated system

A.Nikolakopoulos, A.Lovato, NR, arXiv:2304.11772

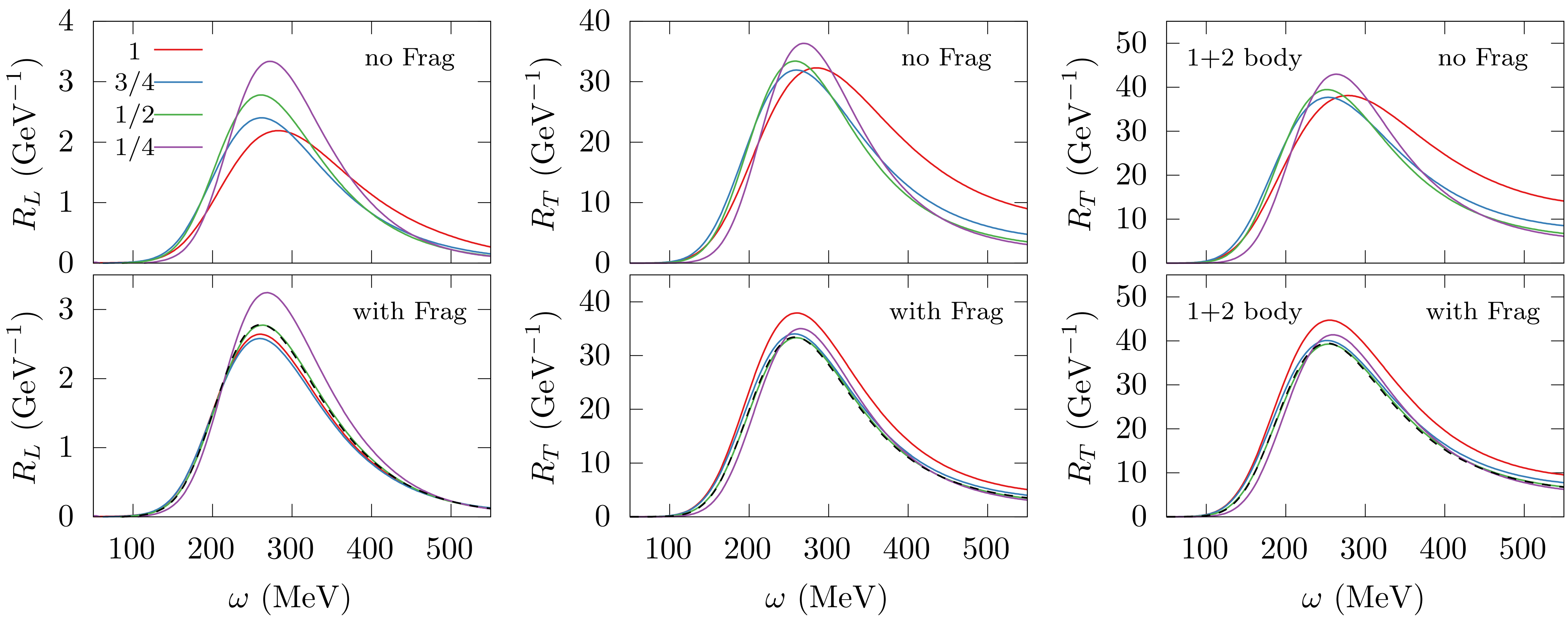

ζ=1/2 Active nucleon Breit frame

Minimizes momentum of incoming and outgoing nucleons

$\mathbf{p}^{fr}_{i} \simeq -\mathbf{q}^{fr}/2$, $\mathbf{p}^{fr}_{f} \simeq \mathbf{q}^{fr}/2$

$$\omega_{QE} = \omega^{nr}_{QE} = 0$$

Two-fragment model

Reduces the frame dependence ⇒includes relativistic corrections kinematics

Final results ≡ ANB calculation

Cross sections: Green’s Function Monte Carlo

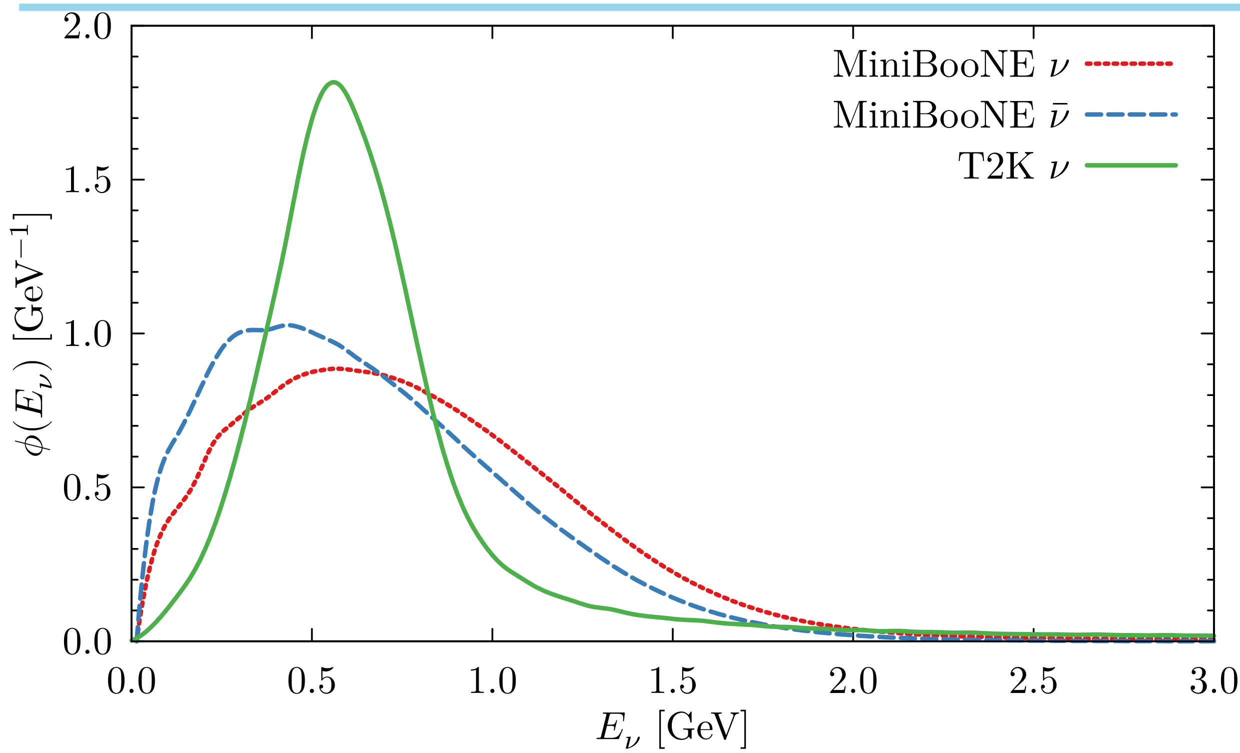

First microscopic calculation of neutrino-nucleus cross section

$$\left\langle \frac{d\sigma}{dT_\mu \, d\cos\theta_\mu} \right\rangle = \int dE_\nu \, \phi(E_\nu) \, \frac{d\sigma(E_\nu)}{dT_\mu \, d\cos\theta_\mu}$$

A. Lovato, NR et al , Phys. Rev. X. 10 (2020) 3, 031068

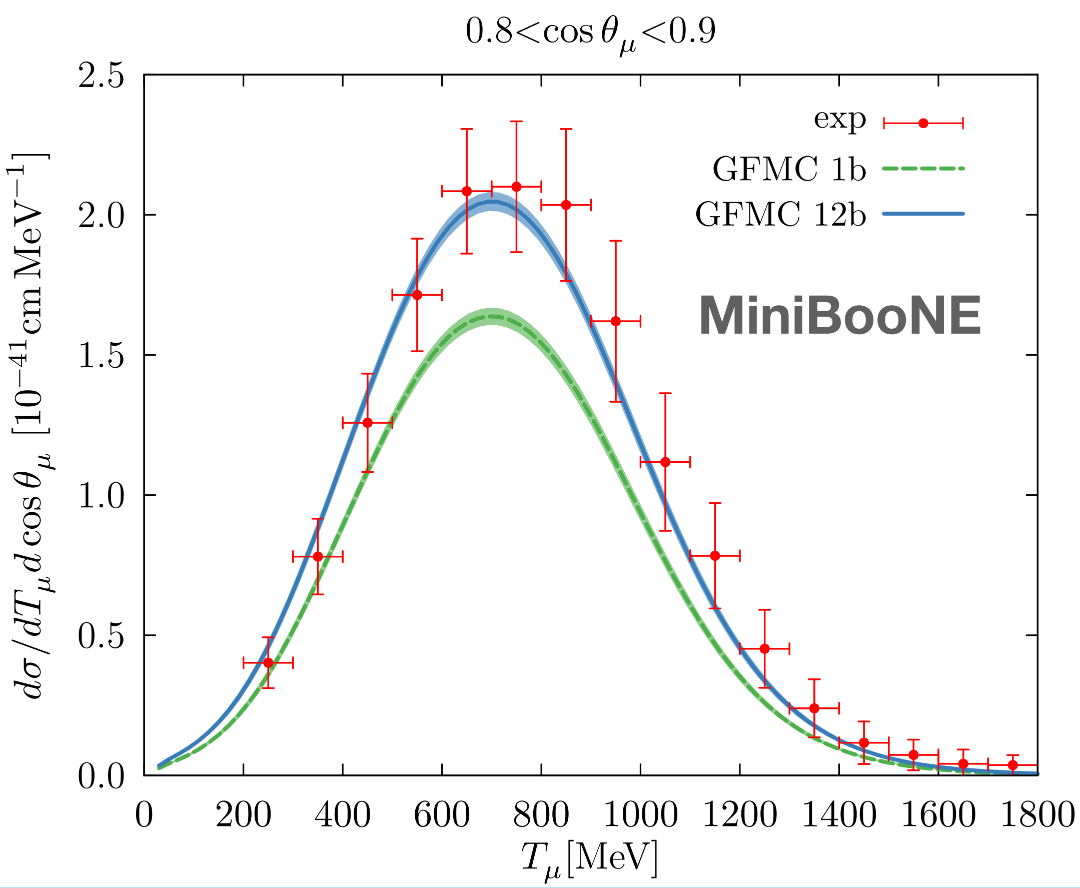

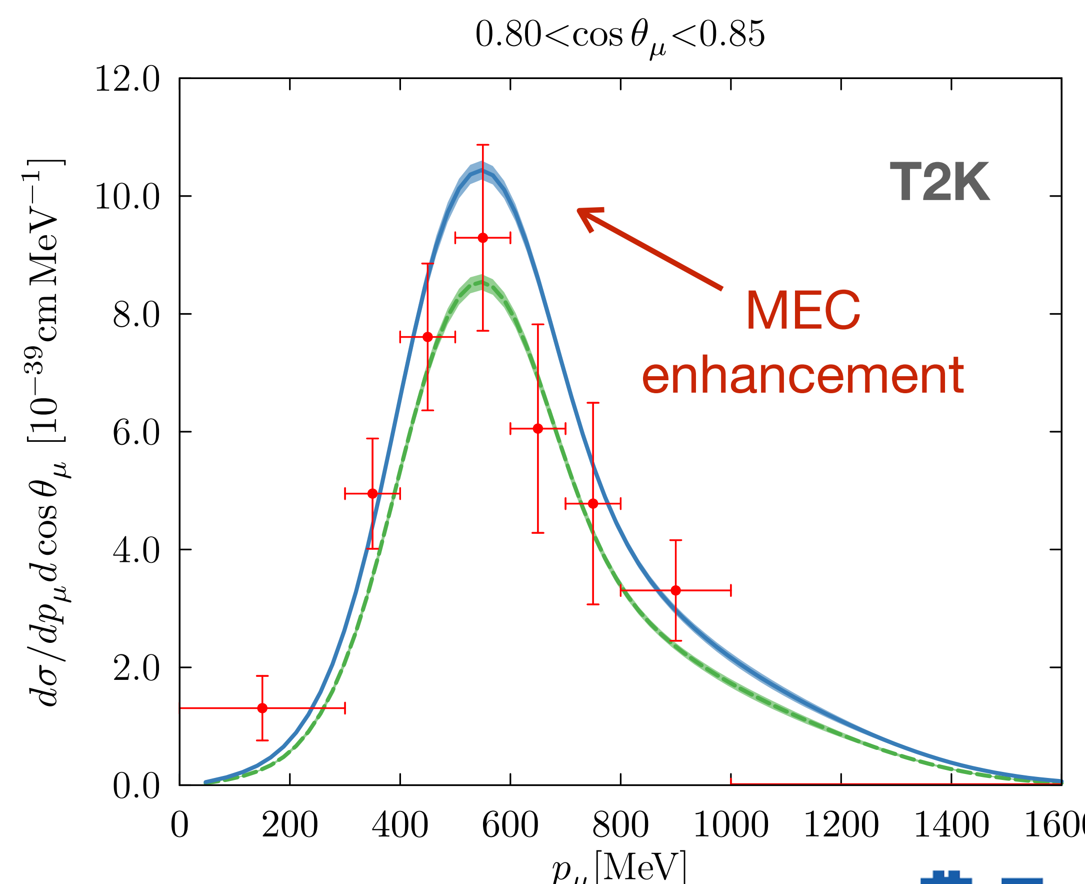

Cross sections: Green's Function Monte Carlo

T2K results including relativistic corrections

A.Nikolakopoulos, A.Lovato, NR, arXiv:2304.11772

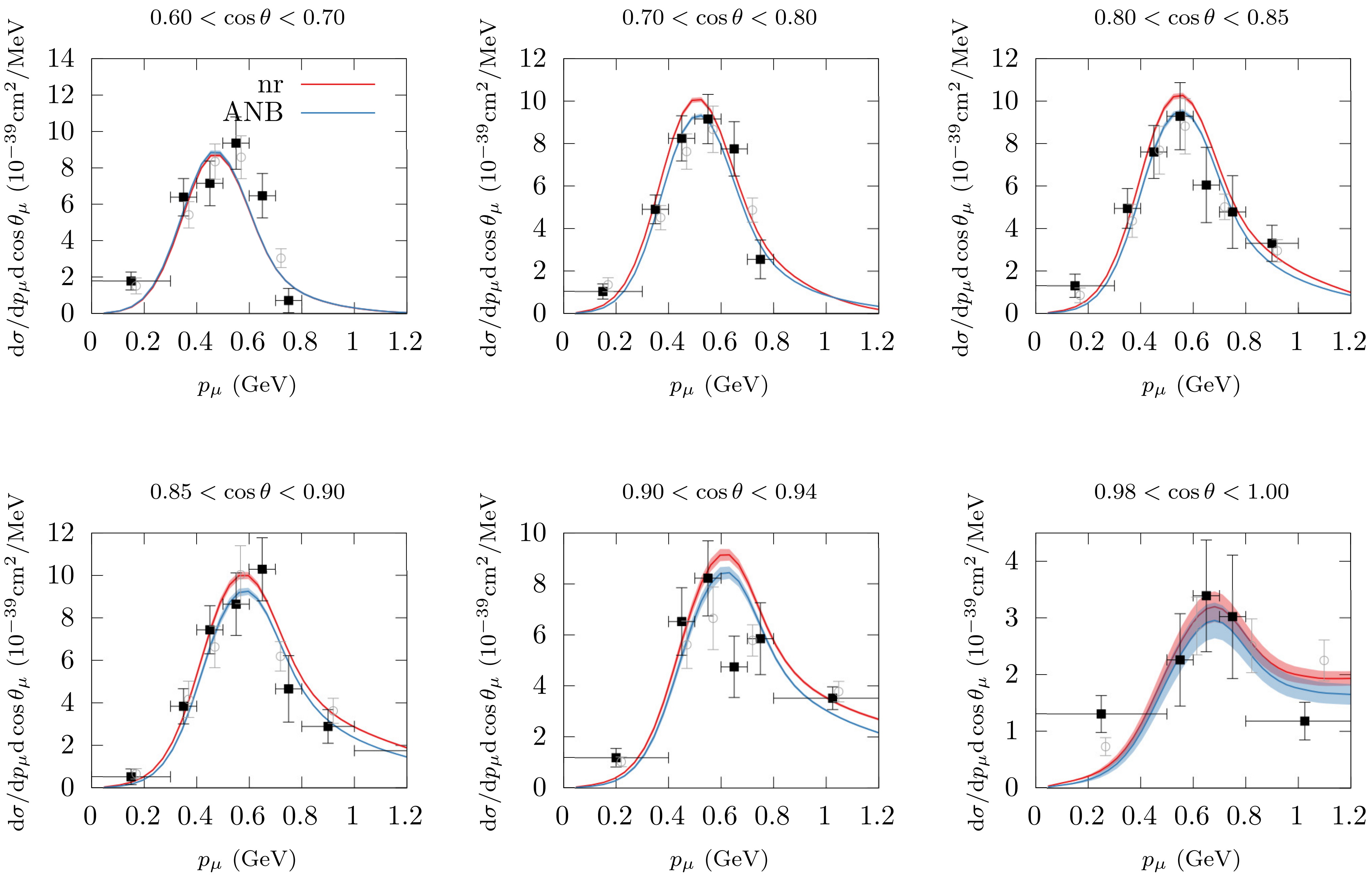

Noemi Rocco, nrocco@fnal.gov

Cross sections: Green's Function Monte Carlo

MiniBooNE results including relativistic corrections

A.Nikolakopoulos, A.Lovato, NR, arXiv:2304.11772

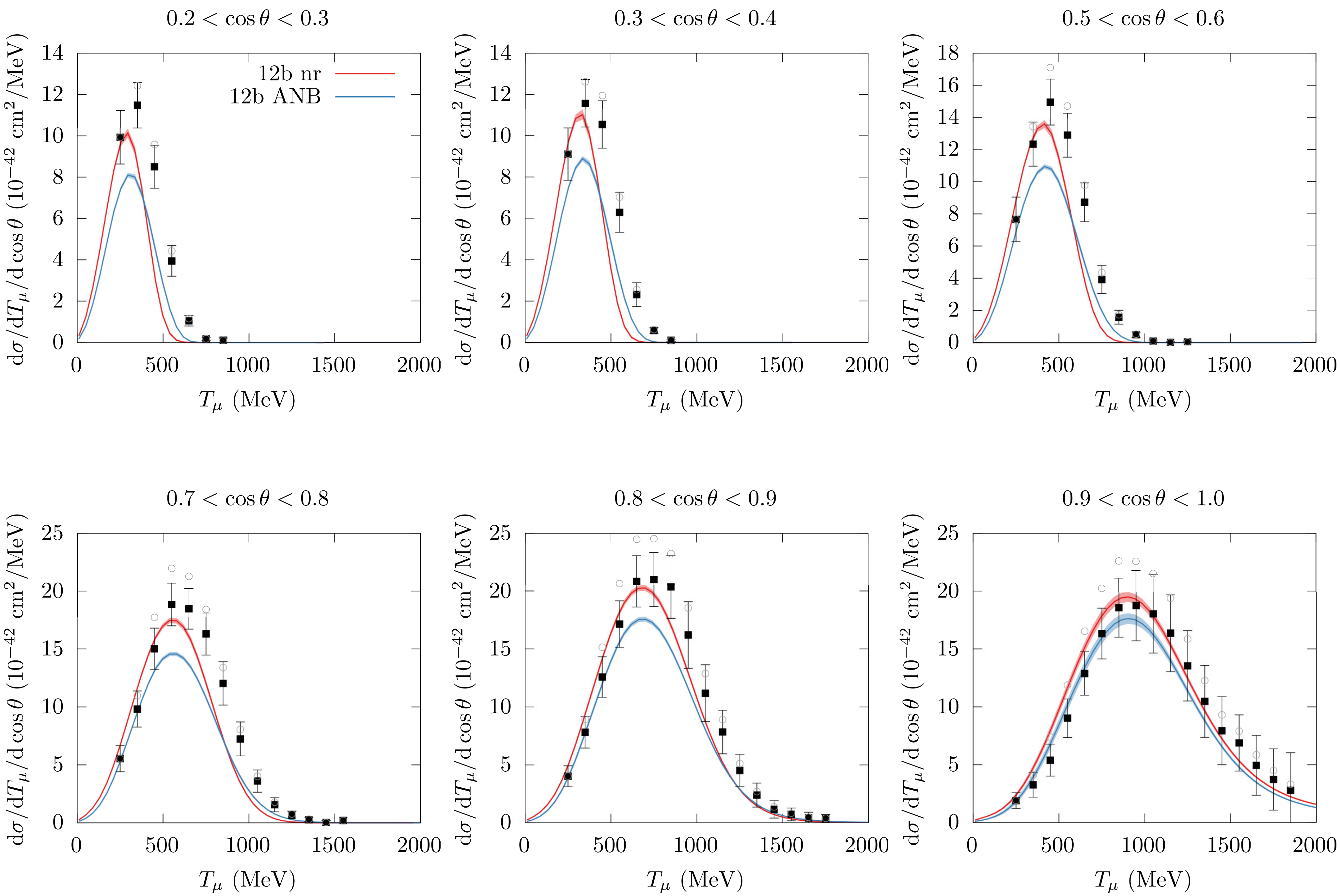

Noemi Rocco, nrocco@fnal.gov

Fermilab

Cross sections: Green's Function Monte Carlo

Electron scattering results including relativistic corrections for some kinematics covered by the calculated responses

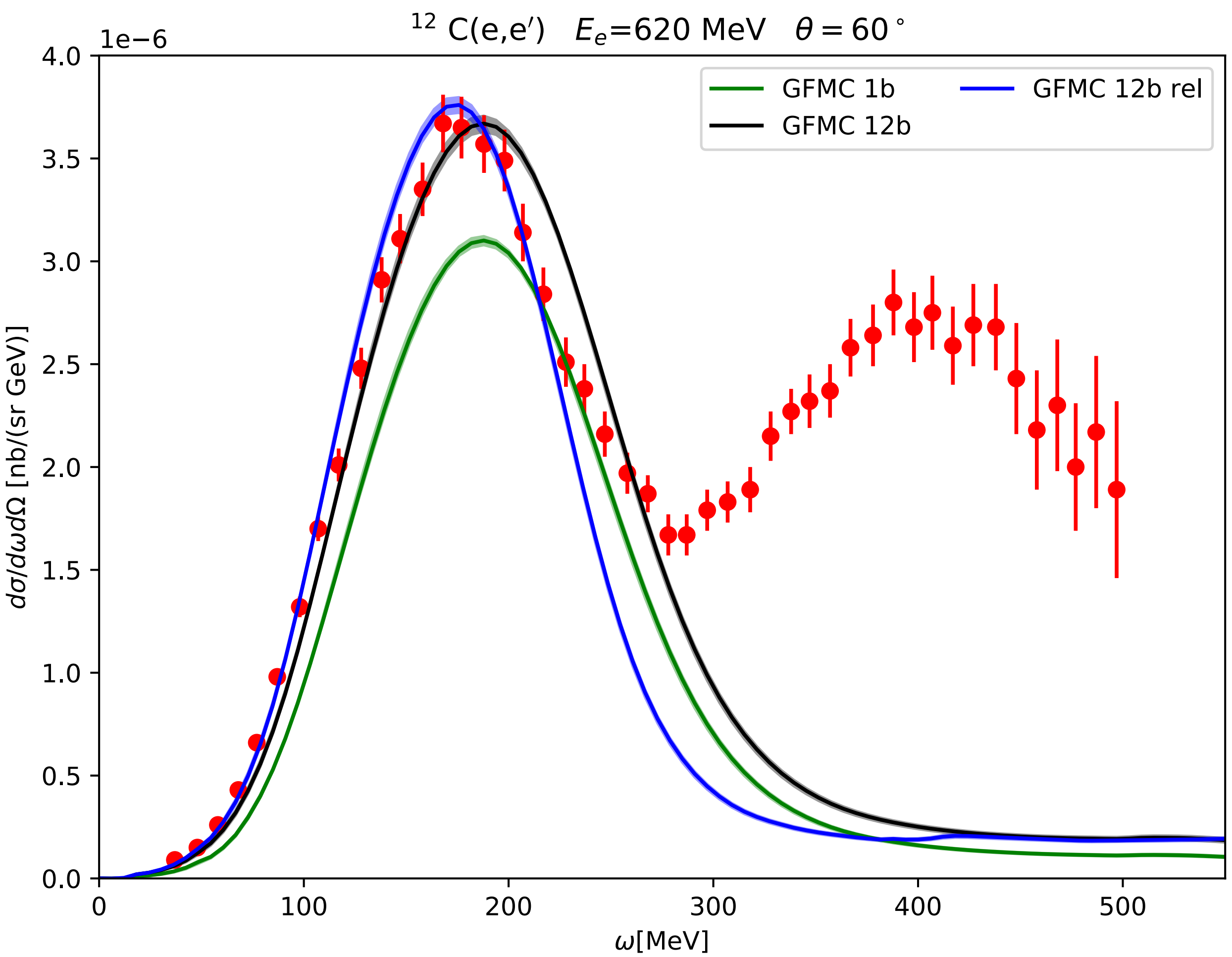

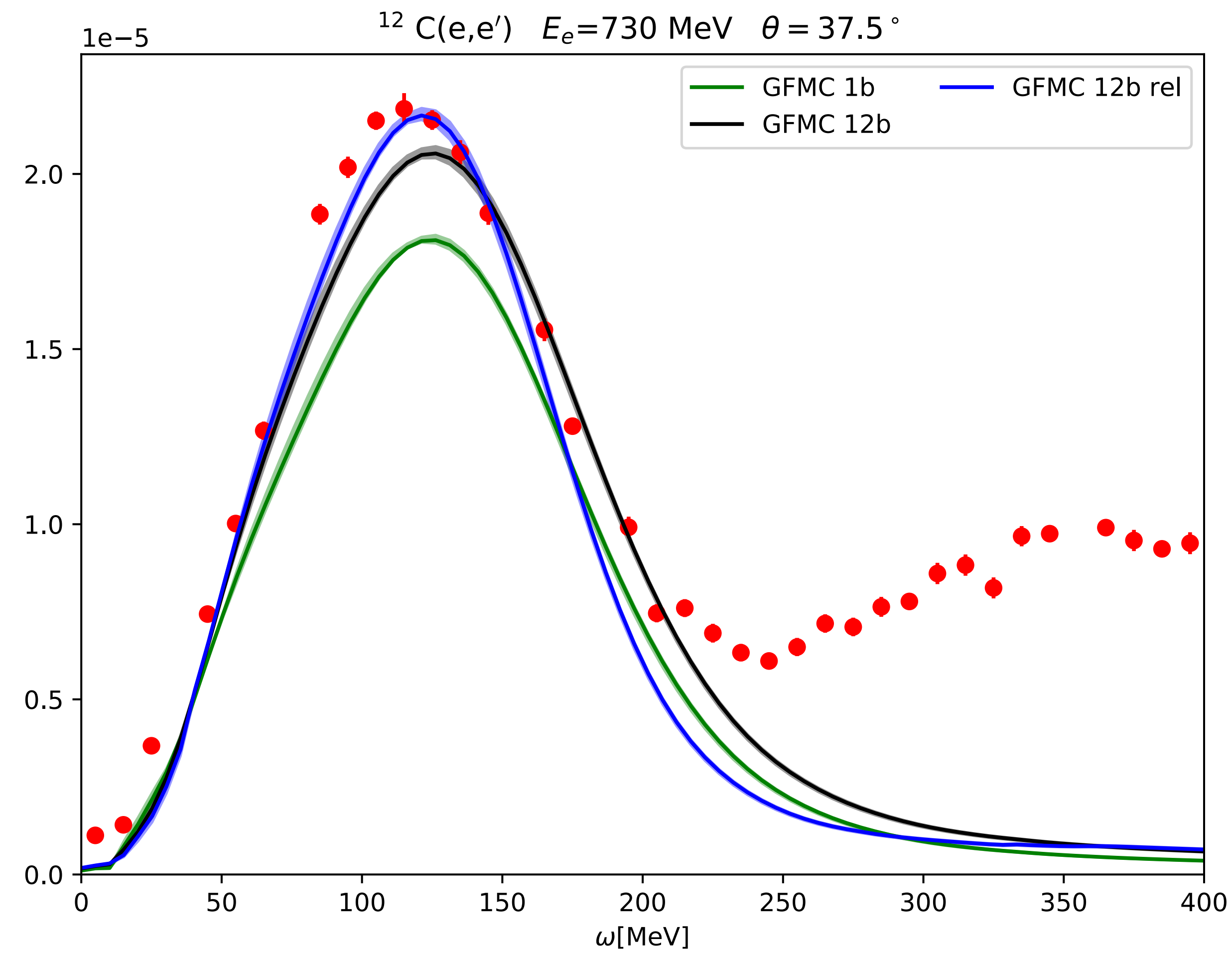

A.Lovato, A.Nikolakopoulos, NR, N. Steinberg, *submitted to Universe*

Addressing Neutrino-Oscillation Physics

J.A. Formaggio and G.P. Zeller, Rev. Mod. Phys. 84 (2012)

Unprecedented accuracy in the determination of **neutrino-argon cross section** is required to achieve design sensitivity to CP violation at DUNE

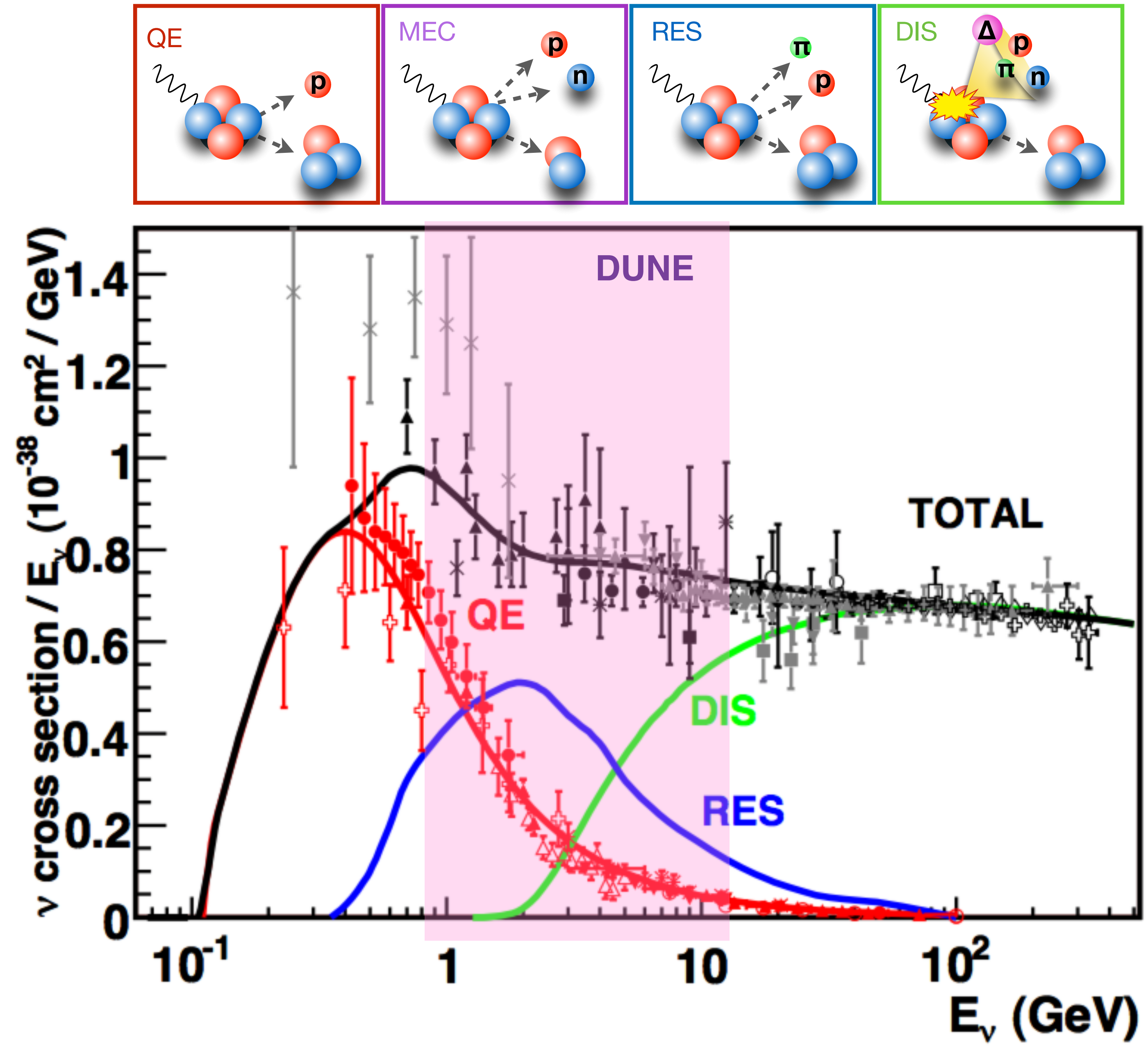

More than 60% of the interactions at DUNE are non-quasielastic

Theoretical tools for neutrino scattering, Contribution to: 2022 Snowmass Summer Study

Noemi Rocco, nrocco@fnal.gov

Cross sections: Spectral function approach

For sufficiently large values of |**q**|, the **factorization scheme** can be applied under the assumptions

$$|\Psi_f\rangle \to |p\rangle \otimes |\Psi_f\rangle_{A-1}$$

$$J_\alpha = \sum_i j^i_\alpha$$

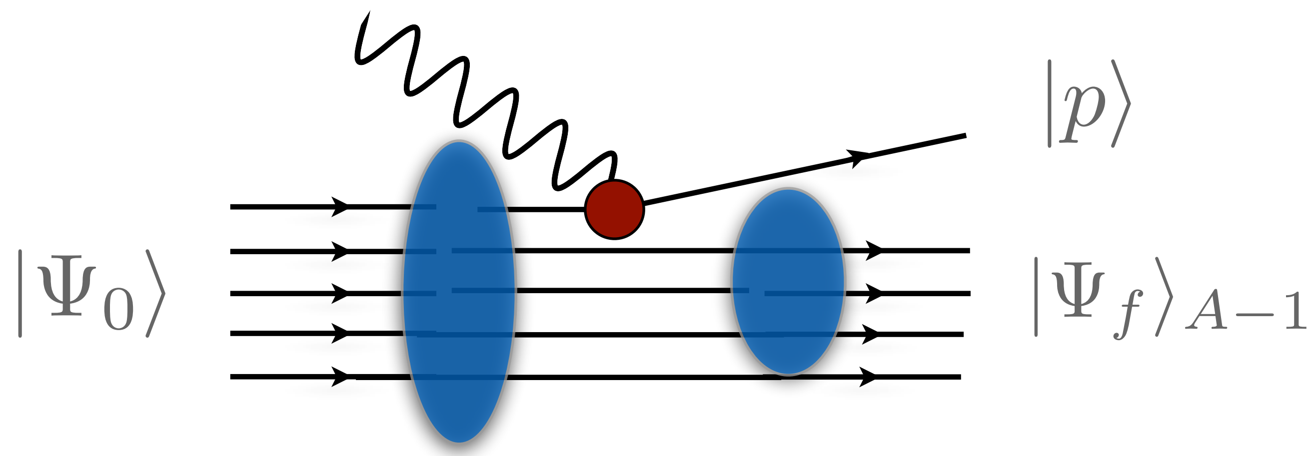

The nuclear cross section is given in terms of the one describing the interaction with individual bound nucleons

$$\boxed{d\sigma_A = \int dE d^3k \; d\sigma_N P(\mathbf{k}, E)}$$

The intrinsic properties of the nucleus are described by the **Spectral Function**→ EFT and nuclear many-body methods

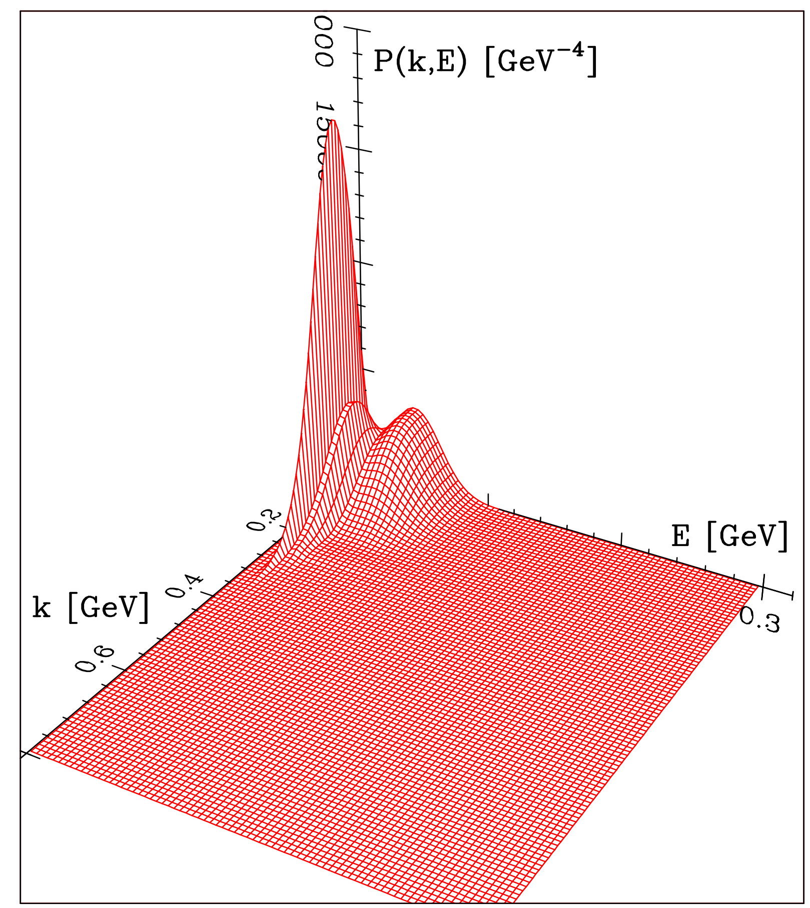

O. Benhar et al, Rev.Mod.Phys. 80 (2008)

Noemi Rocco, nrocco@fnal.gov

QMC Spectral function of nuclei with A=3,4

- Single-nucleon spectral function:

$$P_{p,n}(\mathbf{k},E)=\sum_n \left|\langle\Psi_0^A|\left[|k\rangle|\Psi_n^{A-1}\rangle\right]\right|^2$$
$$\times\,\delta(E+E_0^A-E_n^{A-1})$$
$$=P^{MF}(\mathbf{k},E)+P^{corr}(\mathbf{k},E)$$

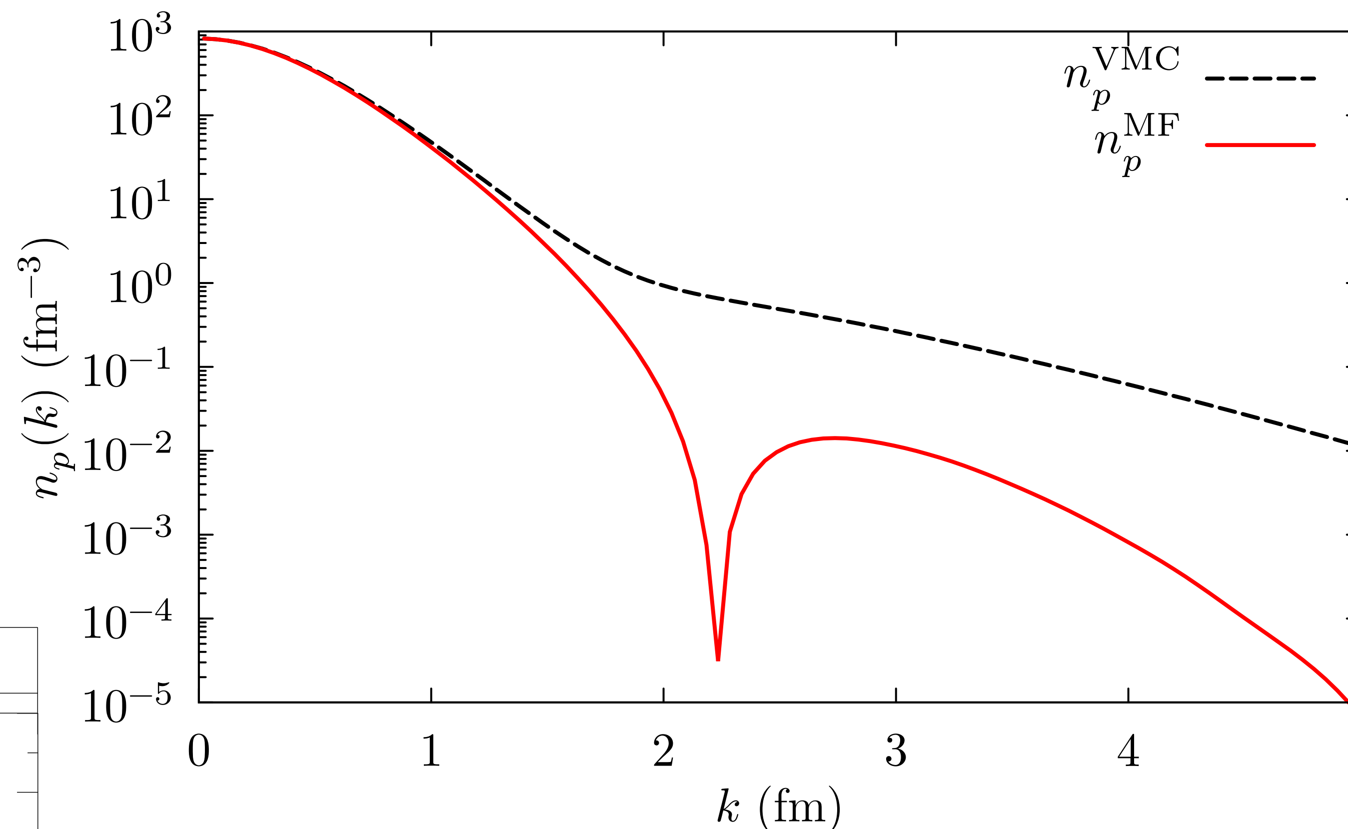

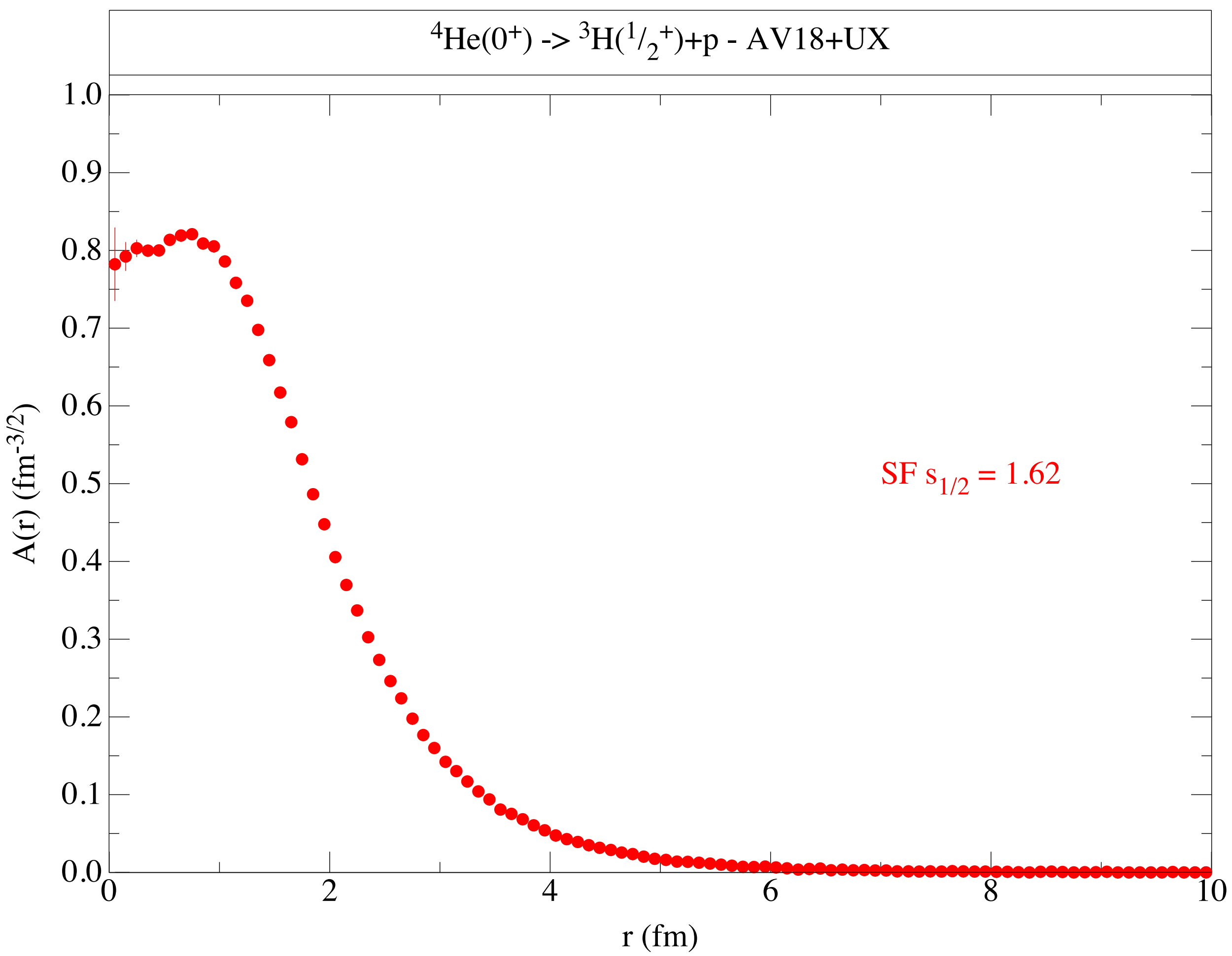

$$P_p^{\rm MF}(\mathbf{k},E)=n_p^{\rm MF}(\mathbf{k})\,\delta\left(E-B_{^4\rm He}+B_{^3\rm H}-\frac{k^2}{2m_{^3\rm H}}\right)$$

$$|\langle\Psi_0^{^4\rm He}|[|k\rangle\otimes|\Psi_0^{^3\rm H}\rangle]|^2$$

- The single-nucleon overlap has been computed within VMC (center of mass motion fully accounted for)

Noemi Rocco, nrocco@fnal.gov

QMC Spectral function of nuclei with A=3,4

$$P_p^{\rm corr}(\mathbf{k},E)=\sum_n\int\frac{d^3k'}{(2\pi)^3}|\langle\Psi_0^A|[|k\rangle\,|k'\rangle\,|\Psi_n^{A-2}\rangle]|^2\delta(E+E_0^A-e(\mathbf{k}')-E_n^{A-2})$$

$$\sum_{\tau_{k'}=p,n} n_{p,\tau_{k'}}(\mathbf{k},\mathbf{k}')\delta\Big(E-B_{^4\mathrm{He}}-e(\mathbf{k}')+B_{A-2}-\frac{(\mathbf{k}+\mathbf{k}')^2}{2m_{A-2}}\Big)$$

Only SRC pairs should be considered: $|\psi_0^{^3H}\rangle$ and $|k'\rangle|\psi_n^{A-2}\rangle$ be orthogonalized

We introduce **cuts** on the **relative distance** between the particles in the two-body momentum distribution

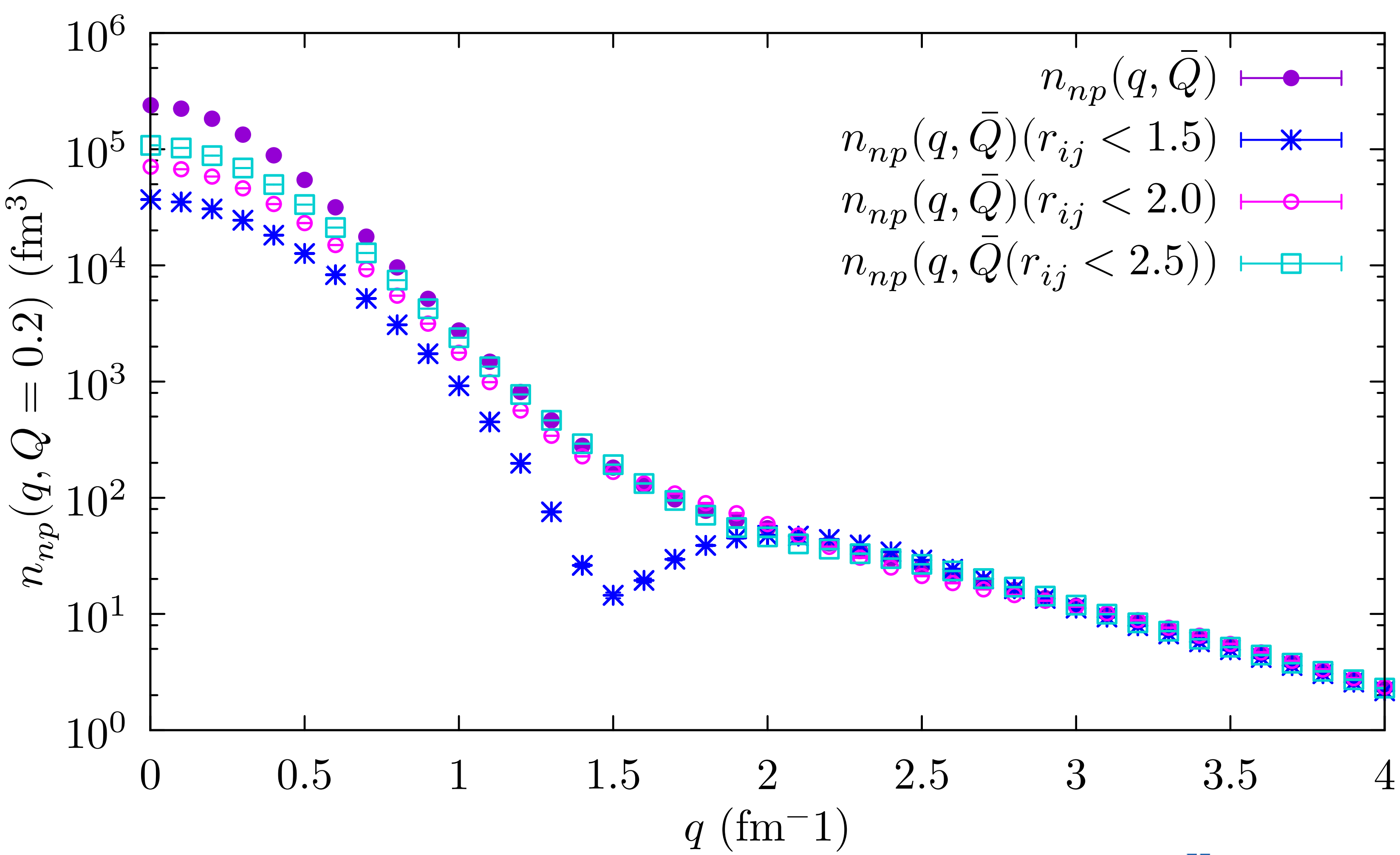

Fermilab

Noemi Rocco, nrocco@fnal.gov

QMC Spectral Function of ^{12}C

- The p-shell contribution has been obtained by FT the radial overlaps:

$$^{12}\mathrm{C}(0^+) \rightarrow ^{11}\mathrm{B}(3/2^-) + p$$
$$^{12}\mathrm{C}(0^+) \rightarrow ^{11}\mathrm{B}(1/2^-) + p$$
$$^{12}\mathrm{C}(0^+) \rightarrow ^{11}\mathrm{B}(3/2^-)^* + p\,.$$

R. Crespo, et al, Phys.Lett.B 803 (2020) 135355

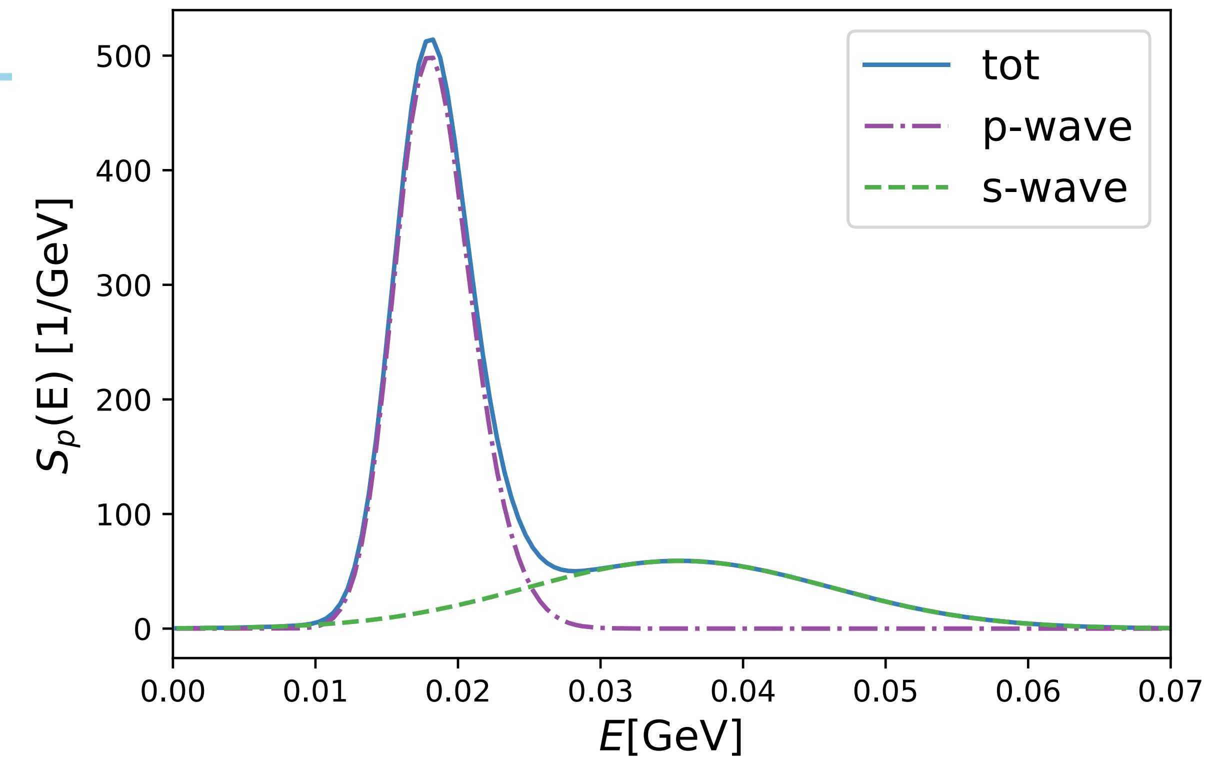

- The quenching of the spectroscopic factors automatically emerges from the VMC calculations

Computing the s-shell contribution is non trivial within VMC. We explored different alternatives:

- Quenched Harmonic Oscillator
- Quenched Wood Saxon
- VMC overlap associated for the $^4\mathrm{He}(0^+) \rightarrow\, ^3\mathrm{H}(1/2^+) + p$ transition

Korover, et al, CLAS collaboration submitted (2021)

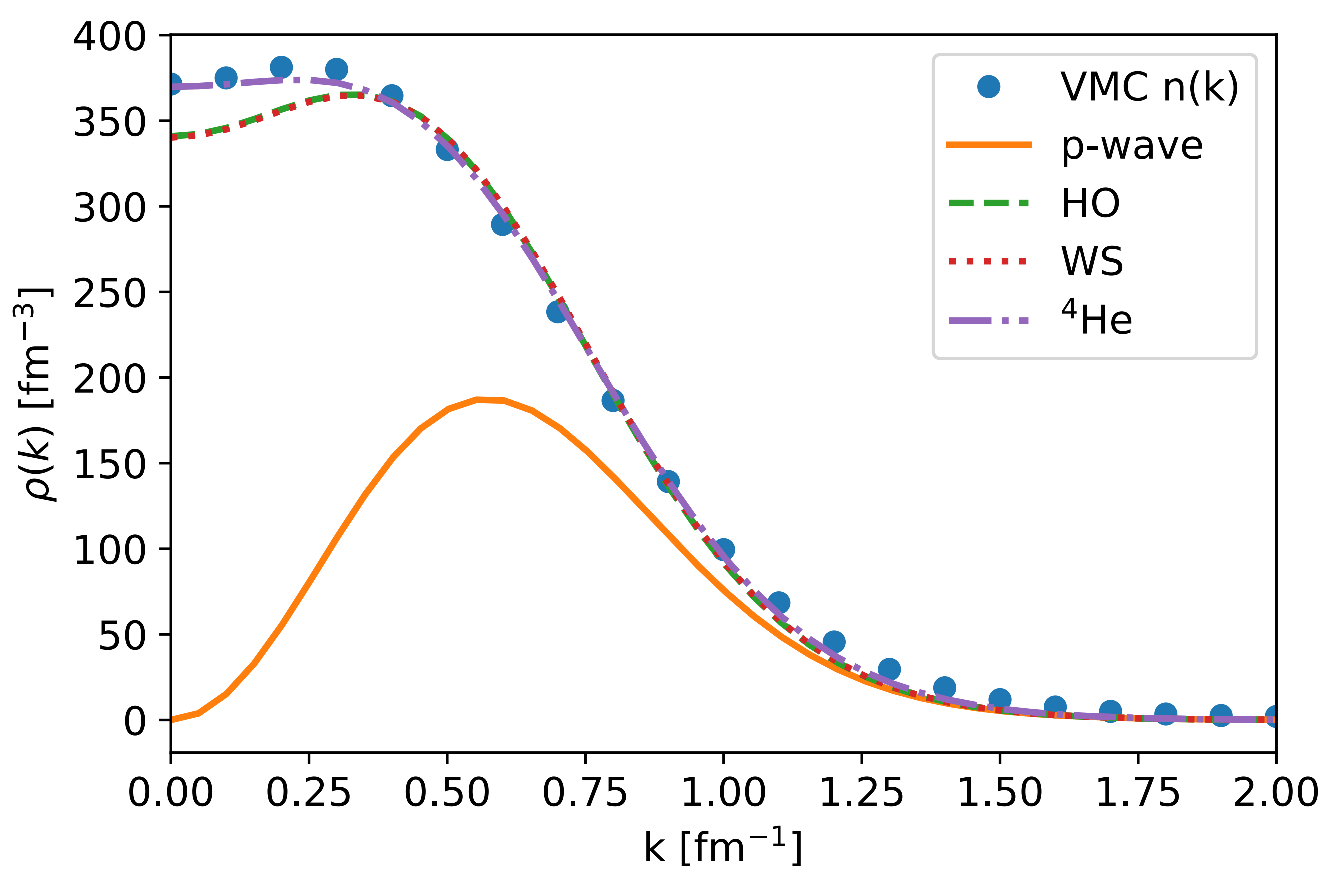

Noemi Rocco, nrocco@fnal.gov

Extended Factorization Scheme

$$\boxed{|f\rangle \to |pp'\rangle_a \otimes |f_{A-2}\rangle} \longrightarrow$$

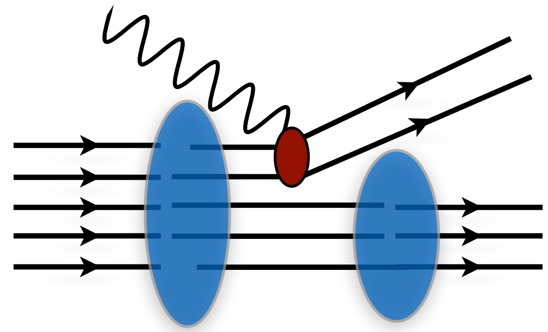

The hadronic tensor for two-body current processes reads

$$W^{\mu\nu}_{2b}(\mathbf{q},\omega) \propto \int dE \frac{d^3k}{(2\pi)^3} \frac{d^3k'}{(2\pi)^3} \frac{d^3p}{(2\pi)^3} P_h(\mathbf{k},\mathbf{k}',E) 2 \sum_{ij} \langle k\, k' | j^{\mu\,\dagger}_{ij} | p\, p'\rangle_a$$
$$\times \langle p\, p' | j^{\nu}_{ij} | k\, k'\rangle \delta(\omega - E + 2m_N - e(\mathbf{p}) - e(\mathbf{p}')) \, .$$

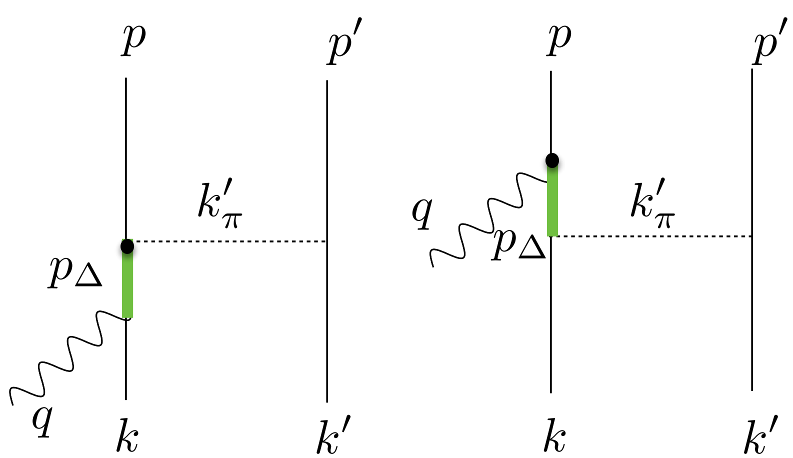

Diagrams including the Delta current depend on many parameters. Axial and vector ff: C_3^V, C_5^A

Delta decay width: $$\Gamma(p_\Delta) = \frac{(4 f_{\pi N\Delta})^2}{12\pi m_\pi^2} \frac{|\mathbf{d}|^3}{\sqrt{s}} (m_N + E_d) R(\mathbf{r}^2)$$

which contains $$R(\mathbf{r}^2) = \left(\frac{\Lambda_R^2}{\Lambda_R^2 - \mathbf{r}^2} \right)$$

 Noemi Rocco, nrocco@fnal.gov

Extended Factorization Scheme

- Production of real π in the final state

$$\boxed{|f\rangle \rightarrow |p_\pi p\rangle \otimes |f_{A-1}\rangle}$$

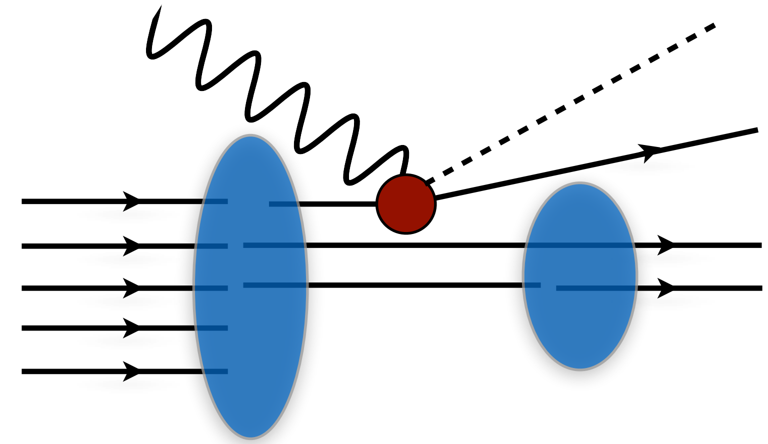

The hadronic tensor for two-body current processes reads

$$W^{\mu\nu}_{1b1\pi}(\mathbf{q},\omega) \propto \int \frac{d^3k}{(2\pi)^3} dE\, P_h(\mathbf{k},E) \frac{d^3p_\pi}{(2\pi)^3} \sum_i \langle k|j_i^{\mu\,\dagger}|p_\pi p\rangle \langle p_\pi p|j_i^\nu|k\rangle$$
$$\times\, \delta(\omega - E + m_N - e(\mathbf{p}) - e_\pi(\mathbf{p}_\pi))$$

Pion production elementary amplitudes derived within the extremely sophisticated **Dynamic Couple Chanel approach**; includes meson baryon channel and nucleon resonances up to W=2 GeV

- The diagrams considered resonant and non resonant π production

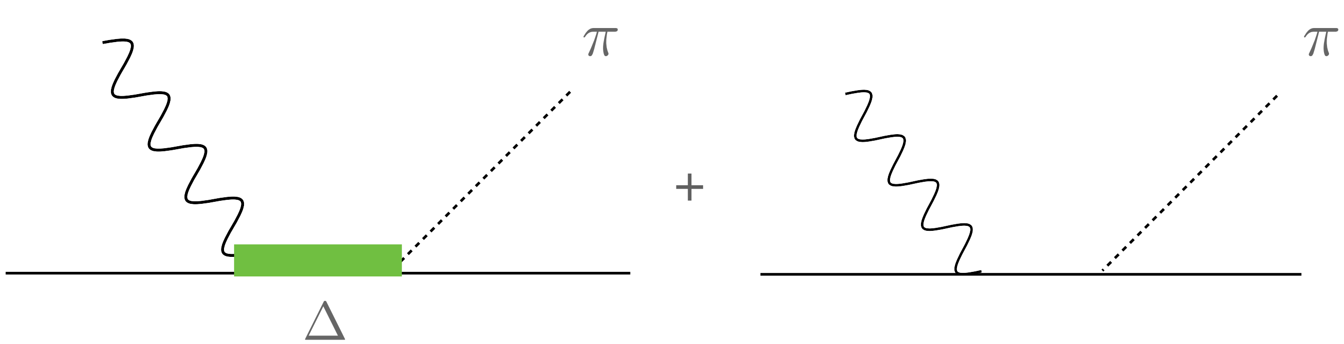

✐ NR, et al, PRC100 (2019) no.4, 045503

✐ H. Kamano et al, PRC 88, 035209 (2013)

✐ S.X.Nakamura et al, PRD 92, 074024 (2015)

Cross sections e^-: Spectral function approach

Spectral function formalism: unified framework able to describe the different reaction mechanisms retaining an accurate treatment of nuclear dynamics

- Good agreement with electron scattering data when all reaction mechanisms are included

NR, Frontiers in Phys. 8 (2020) 116

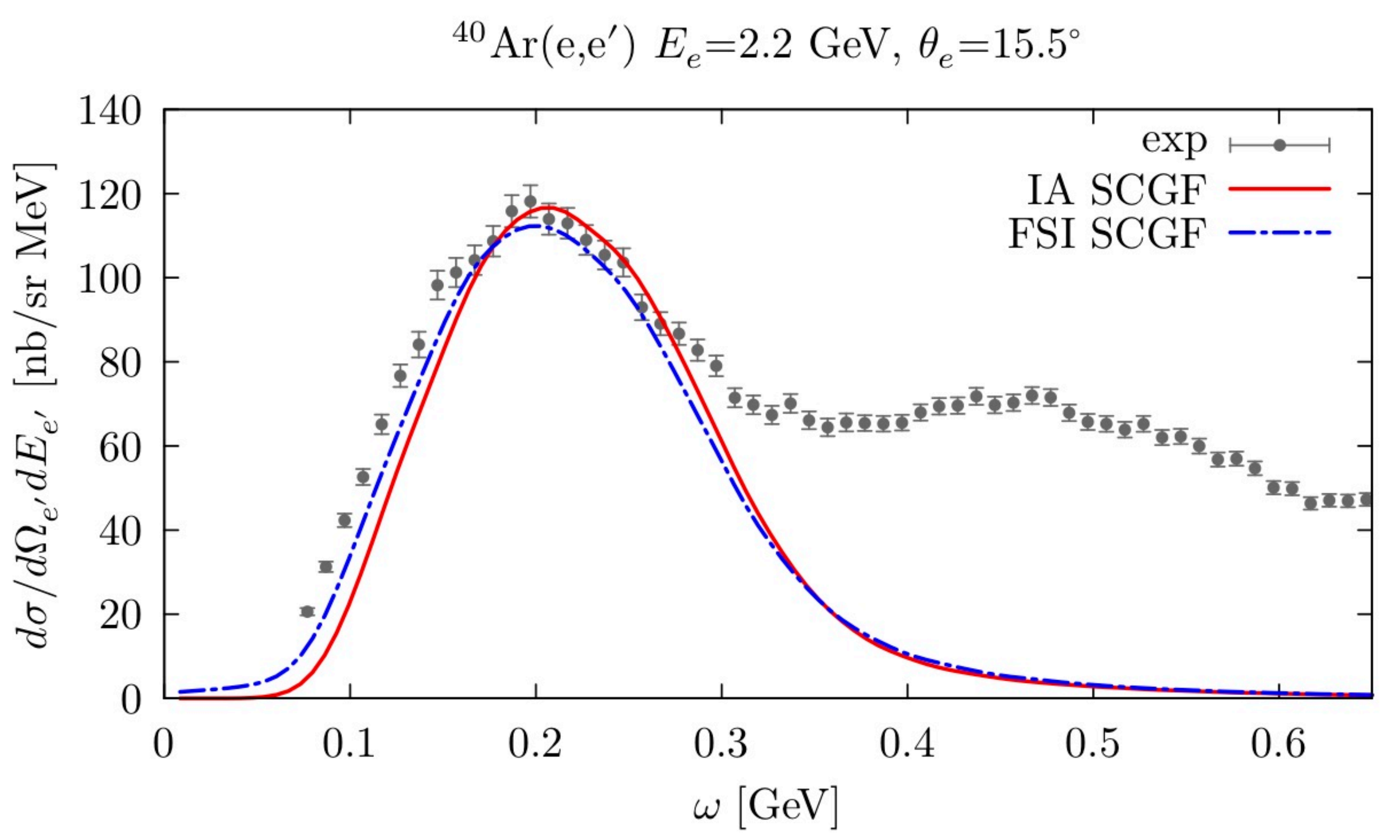

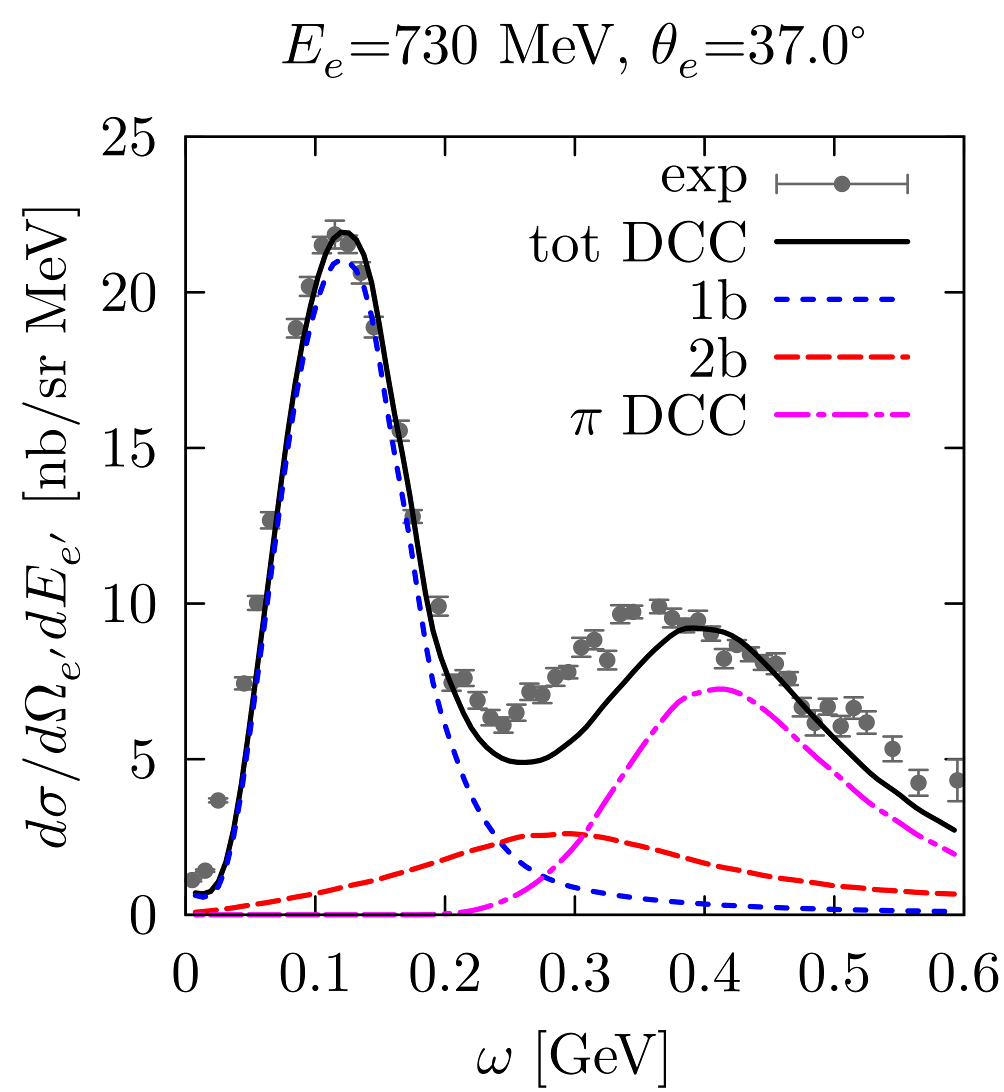

Contributions missing: interference effects, 2π emission, DIS

Comparing different many-body methods

- e -^{3}H: inclusive cross section

L. Andreoli, NR, et al, PRC 105 (2022) 1, 014002

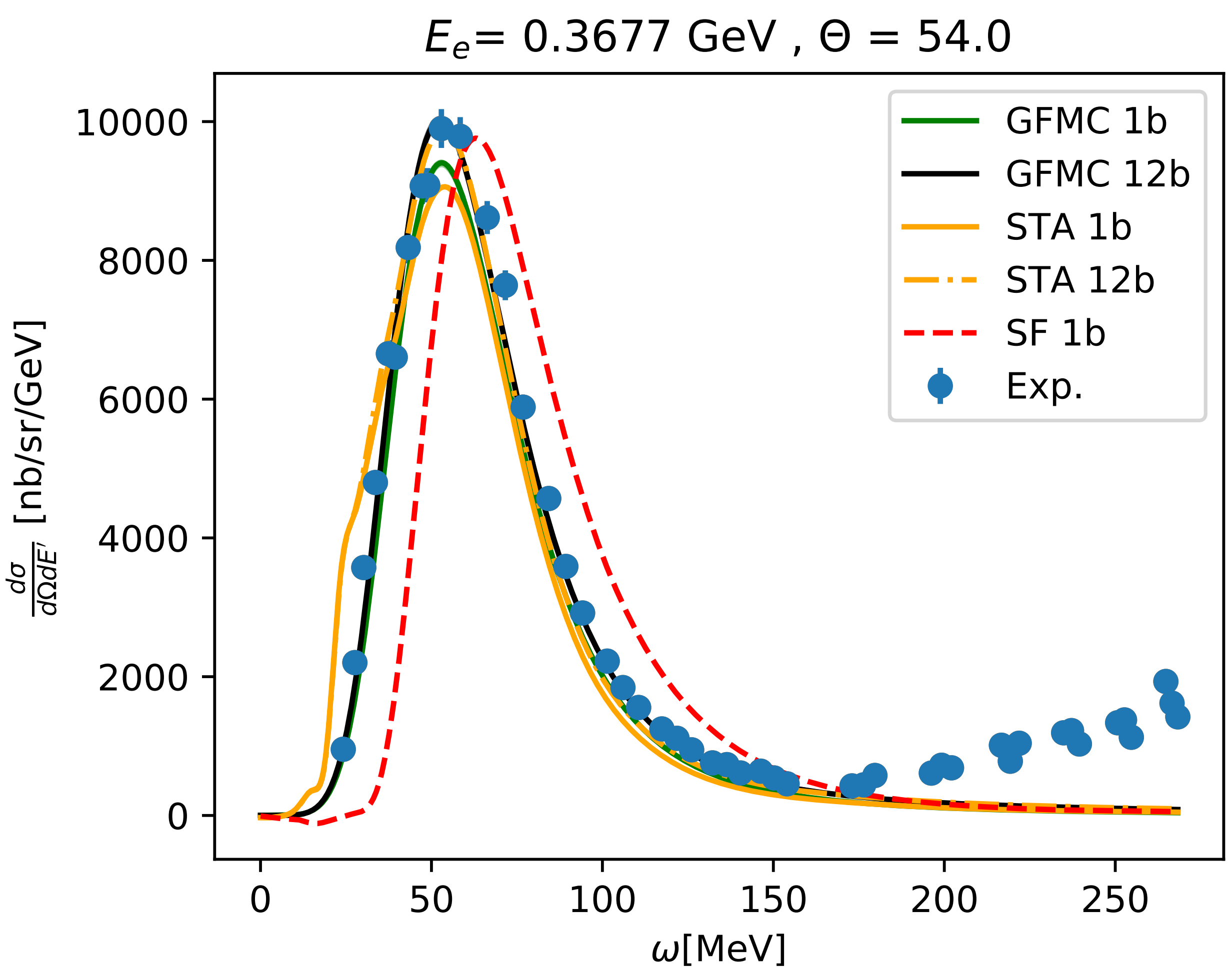

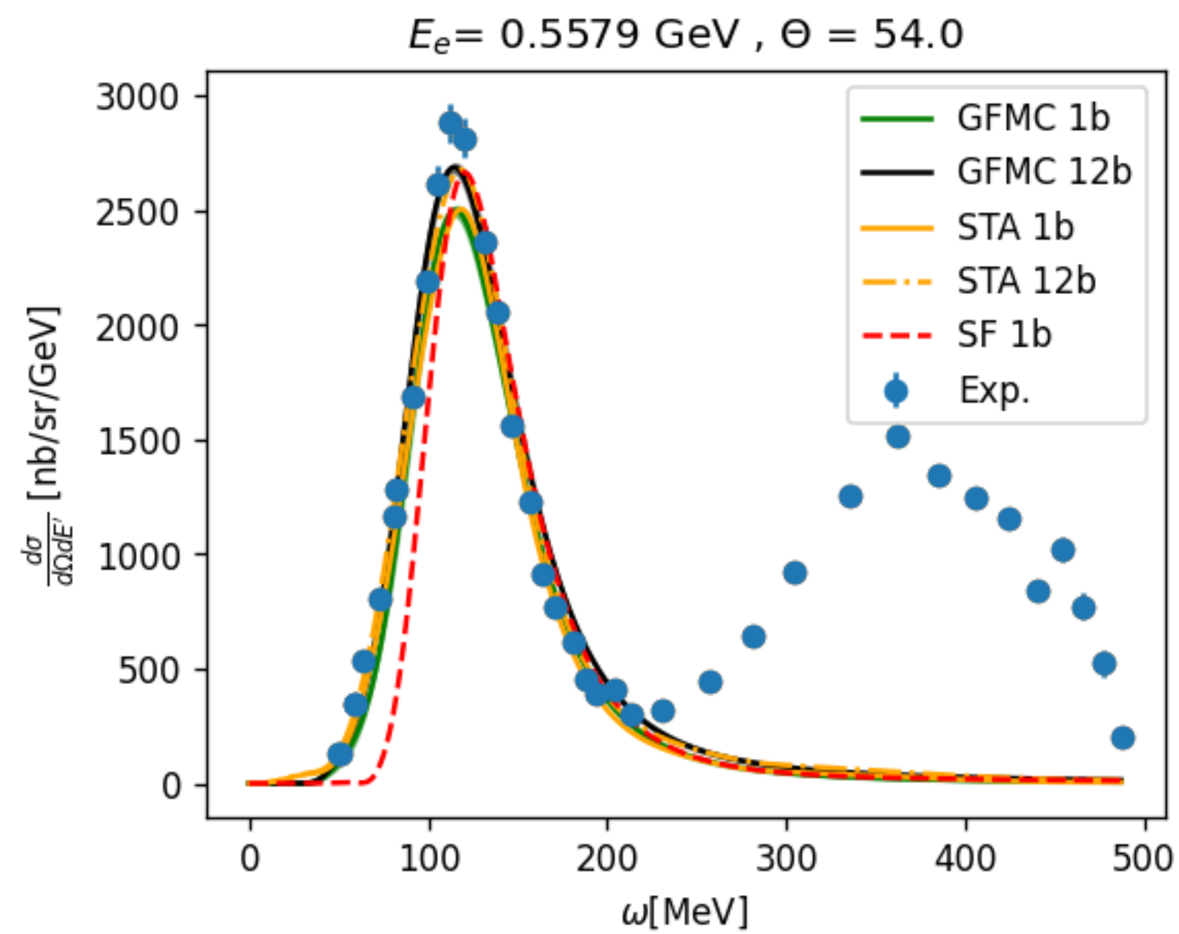

- Comparisons among QMC, SF, and STA approaches: first step to precisely **quantify the uncertainties i**nherent to the factorization of the final state.

- Gauge the role of **relativistic effects** in the energy region relevant for neutrino experiments.

Comparing different many-body methods

MiniBooNE results; breakdown into one- and two-body contributions for the SF and GFMC

D.Simons, N. Steinberg et al
arXiv:2210.02455

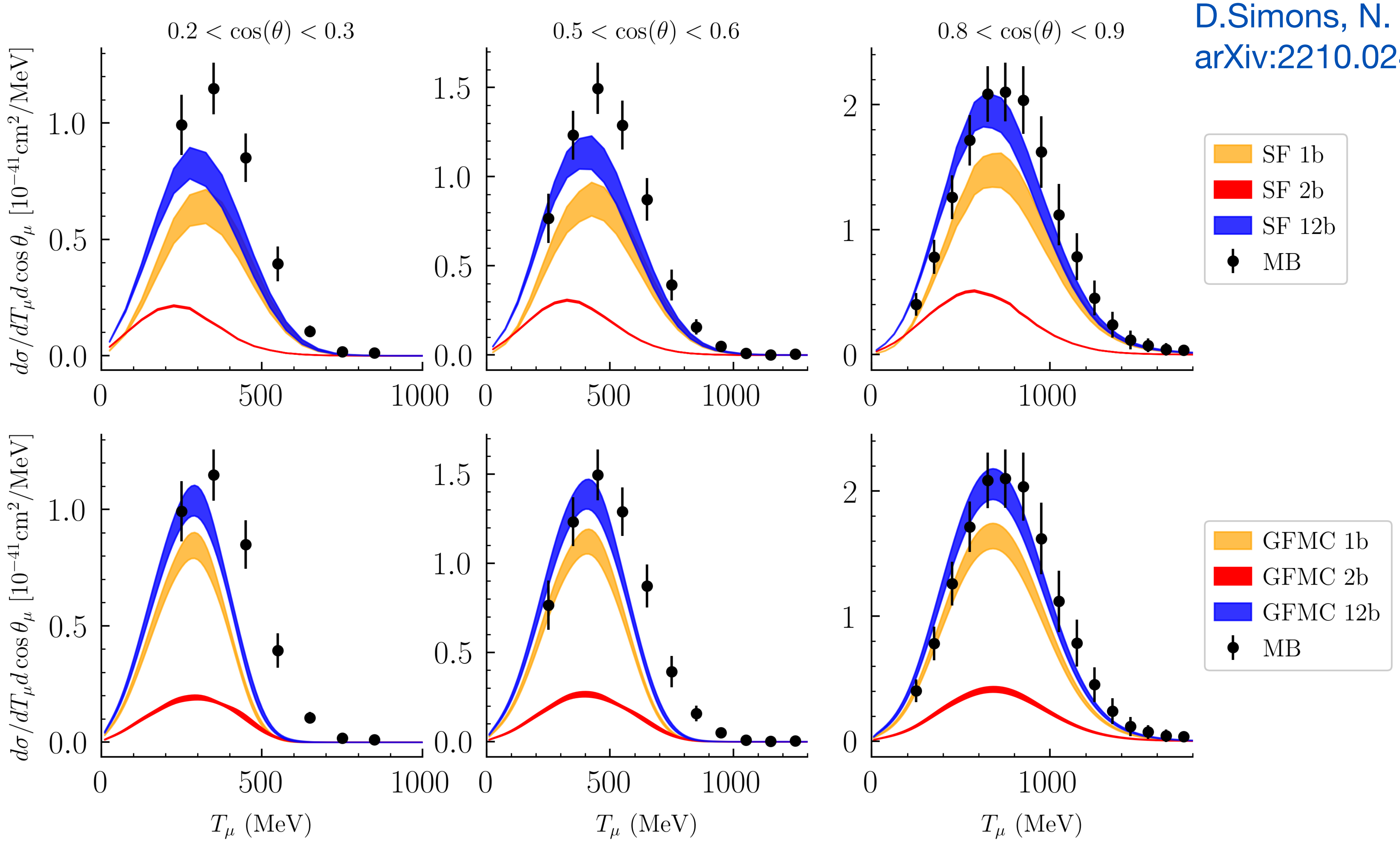

MiniBooNE	$0.2 < \cos\theta_\mu < 0.3$	$0.5 < \cos\theta_\mu < 0.6$	$0.8 < \cos\theta_\mu < 0.9$
GFMC/SF difference in $d\sigma_{\text{peak}}$ (%)	22.8	20.3	5.6

Comparing different many-body methods

T2K results; breakdown into one- and two-body contributions for the SF and GFMC

D.Simons, N. Steinberg et al
arXiv:2210.02455

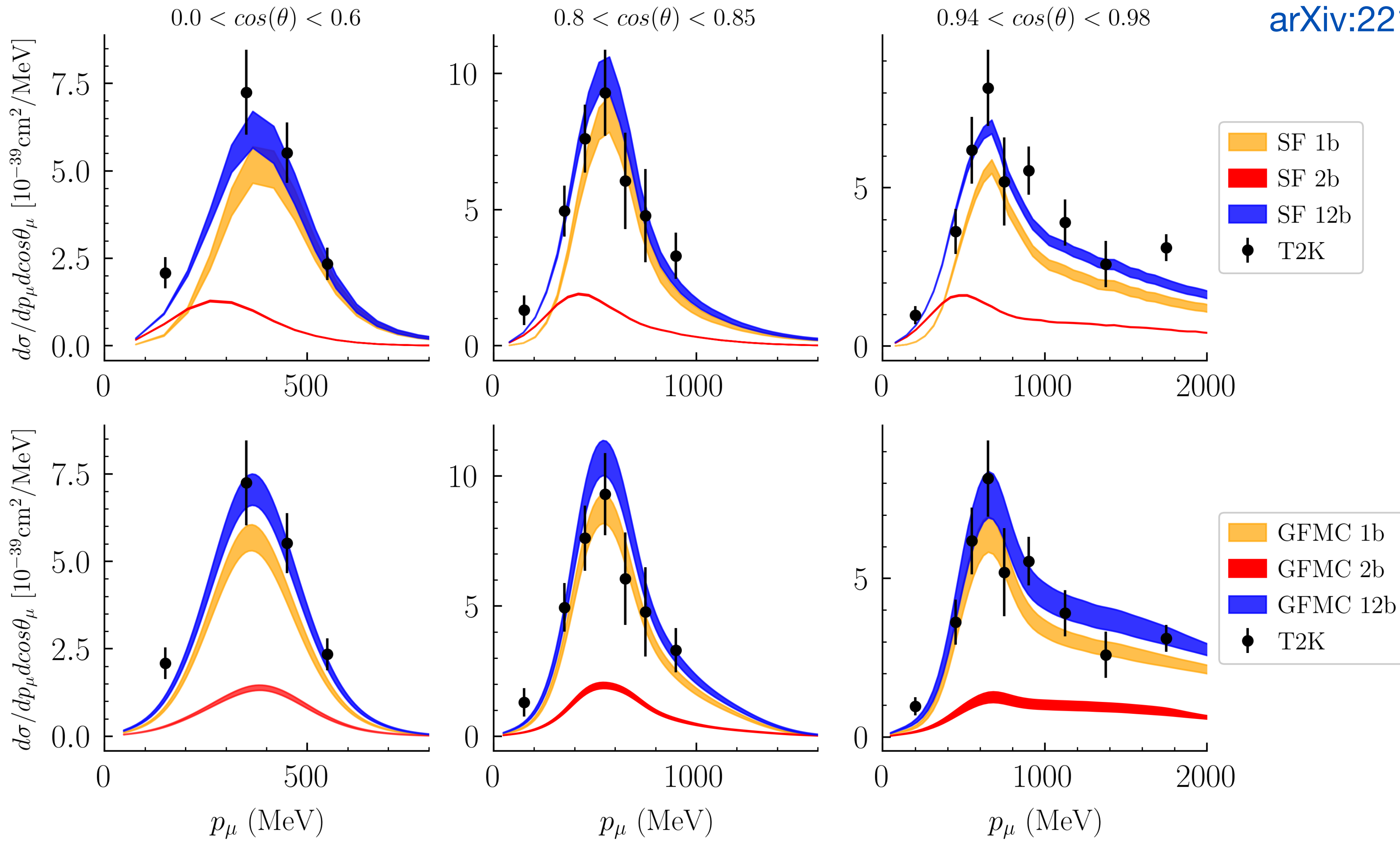

T2K	$0.0 < \cos\theta_\mu < 0.6$	$0.80 < \cos\theta_\mu < 0.85$	$0.94 < \cos\theta_\mu < 0.98$
GFMC/SF difference in $d\sigma_{\text{peak}}$ (%)	13.4	7.3	10.0

Comparing different many-body methods

— MINERvA M.E. Double Differential Cross Section in p_T, $p_{||}$. CCQE-like data on CH

N. Steinberg, A. Nikolakopoulos, A. Lovato, NR, *submitted to Universe*

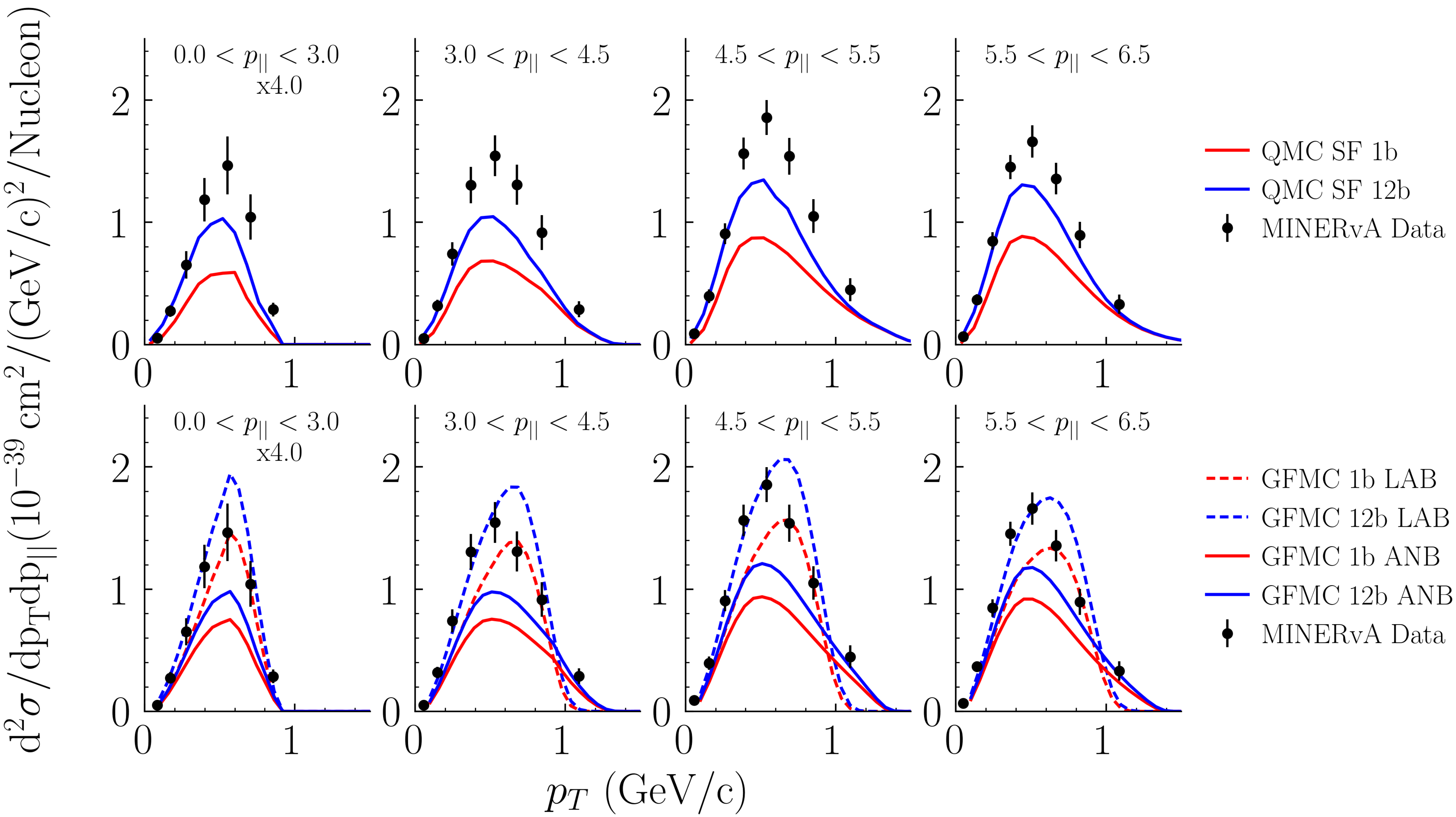

Noemi Rocco, nrocco@fnal.gov

Fermilab

Input parameters and their precision

There is no EFT that coverages over all of DUNE kinematics

The first steps towards getting few-% cross-section uncertainties are understanding what input parameters we will need and what precision we will need them at.

Lattice QCD can provide inputs to be included in EFTs and nuclear many-body methods

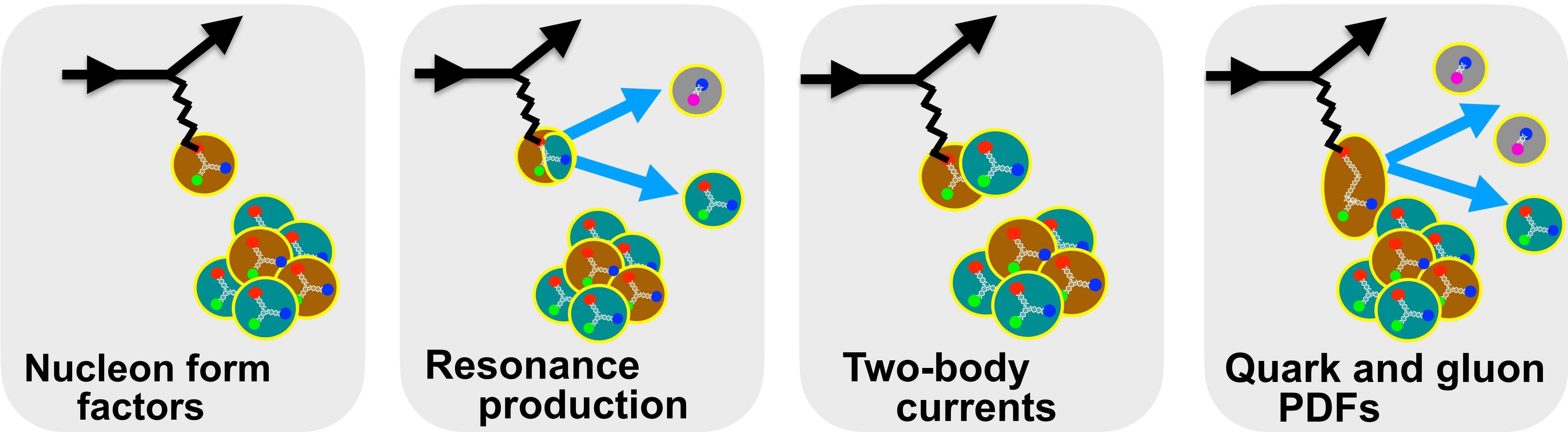

Courtesy of M. Wagman

Noemi Rocco, nrocco@fnal.gov

Elementary Input: Form Factors

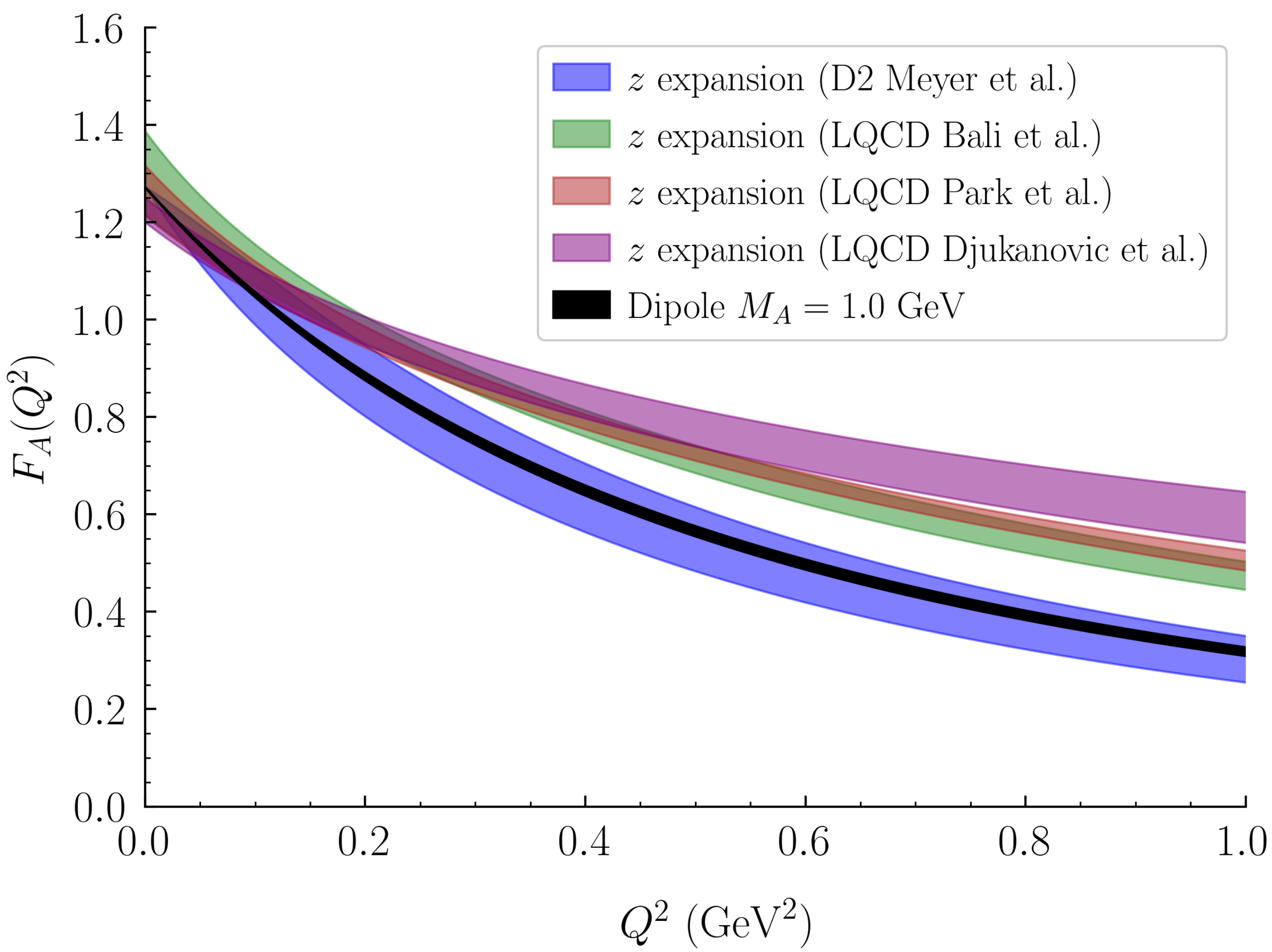

Different parametrization of the axial form factor:

Dipole: $$F_A(Q^2) = \frac{g_A}{(1+Q^2/M_A^2)^2},$$

Different determinations of nucleon axial form factor using the z-expansion

$$F_A(Q^2) = \sum_{k=0}^{\infty} a_k\, z(Q^2)^k \approx \sum_{k=0}^{k_{\max}} a_k\, z(Q^2)^k,$$

UQ independent on assumptions about the shape of the axial form factor.

D2 Meyer et al: fits to neutrino-deuteron scattering data

LQCD result: general agreement between the different calculations

LQCD results are 2-3σ larger than D2 Meyer ones for $Q^2 > 0.3$ GeV^2

Noemi Rocco, nrocco@fnal.gov

Study of model dependence in neutrino predictions

MiniBooNE results; breakdown into one- and two-body contributions for the SF and GFMC

D.Simons, N. Steinberg et al
arXiv:2210.02455

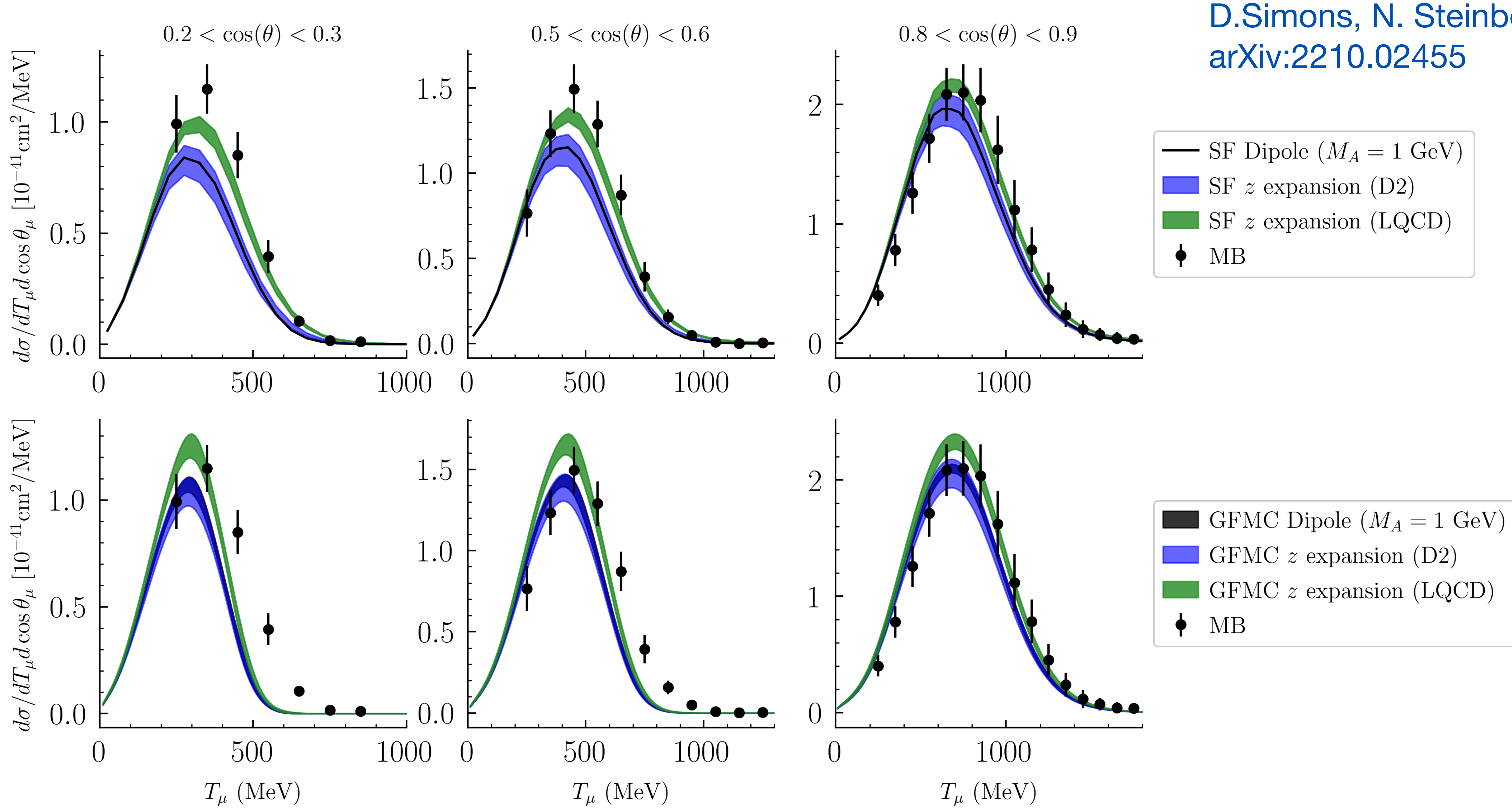

MiniBooNE	$0.2 < \cos\theta_\mu < 0.3$	$0.5 < \cos\theta_\mu < 0.6$	$0.8 < \cos\theta_\mu < 0.9$
SF Difference in $d\sigma_{\text{peak}}$ (%)	16.3	17.1	9.3
GFMC Difference in $d\sigma_{\text{peak}}$ (%)	18.6	17.1	12.2

Noemi Rocco, nrocco@fnal.gov

Study of model dependence in neutrino predictions

T2K results; breakdown into one- and two-body contributions for the SF and GFMC

D.Simons, N. Steinberg et al
arXiv:2210.02455

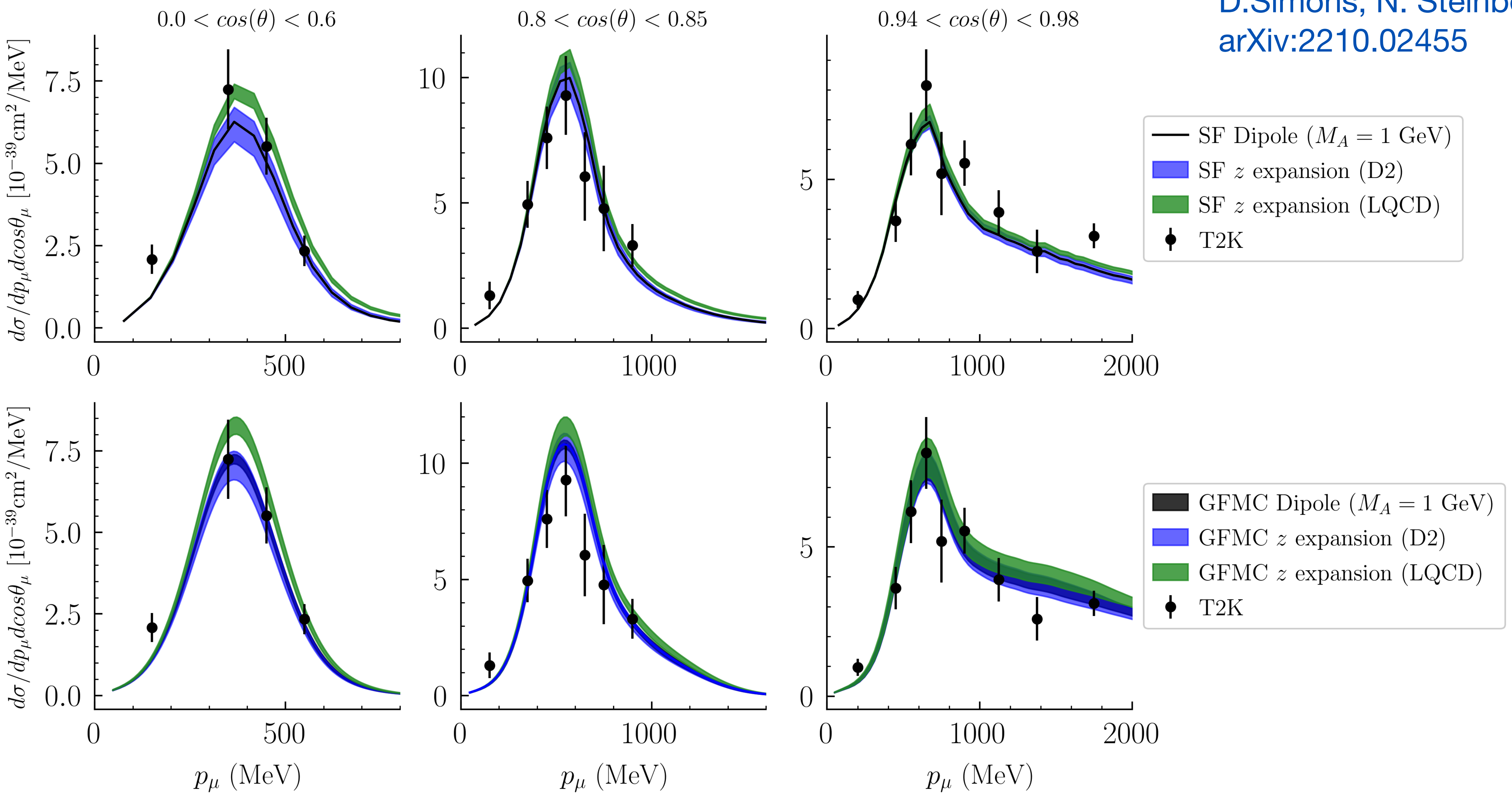

T2K	$0.0 < \cos\theta_\mu < 0.6$	$0.80 < \cos\theta_\mu < 0.85$	$0.94 < \cos\theta_\mu < 0.98$
SF difference in $d\sigma_{\text{peak}}$ (%)	15.3	8.2	3.3
GFMC difference in $d\sigma_{\text{peak}}$ (%)	15.8	8.0	4.6

Noemi Rocco, nrocco@fnal.gov

Delta contribution to MEC

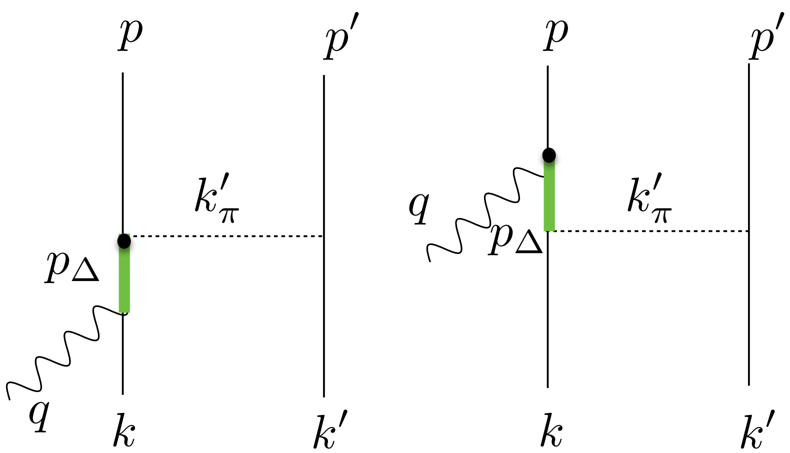

Diagrams including the Delta current depend on many parameters.

$$(j_a^\mu)_A = (k'_\pi)^\alpha G_{\alpha\beta}(p_\Delta)\Big[\frac{C_3^A}{m_N}\Big(g^{\beta\mu}\not{q} - q^\beta\gamma^\mu\Big) + \frac{C_4^A}{m_N^2}\Big(g^{\beta\mu}q\cdot p_\Delta - q^\beta p_\Delta^\mu\Big) + C_5^A g^{\beta\mu} + \frac{C_6^A}{m_N^2}q^\mu q^\alpha\Big],$$

Parametrization chosen for the axial ff:

$$C_5^A = \frac{1.2}{(1-q^2/M_{A\Delta})^2} \times \frac{1}{1-q^2/(3M_{A\Delta})^2)},$$

Current extractions of C_A^5 (0) rely on single pion production data from deuterium bubble chamber experiments; estimated uncertainty ~ 15 %

Delta decay width:

$$\Gamma(p_\Delta) = \frac{(4f_{\pi N\Delta})^2}{12\pi m_\pi^2}\frac{|\mathbf{d}|^3}{\sqrt{s}}(m_N + E_d)R(\mathbf{r}^2)$$

$$R(\mathbf{r}^2) = \left(\frac{\Lambda_R^2}{\Lambda_R^2 - \mathbf{r}^2}\right)$$

Noemi Rocco, nrocco@fnal.gov

Resonance Uncertainty needs

The largest contributions to two-body currents arise from resonant $N \to \Delta$ transitions yielding pion production

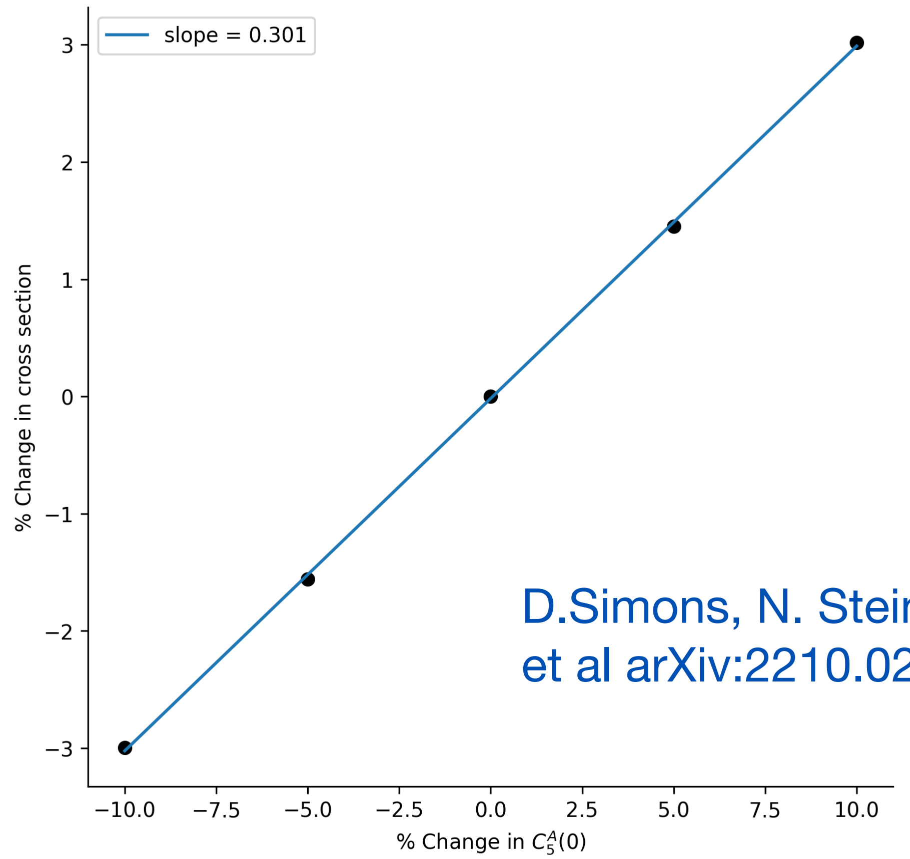

D.Simons, N. Steinberg et al arXiv:2210.02455

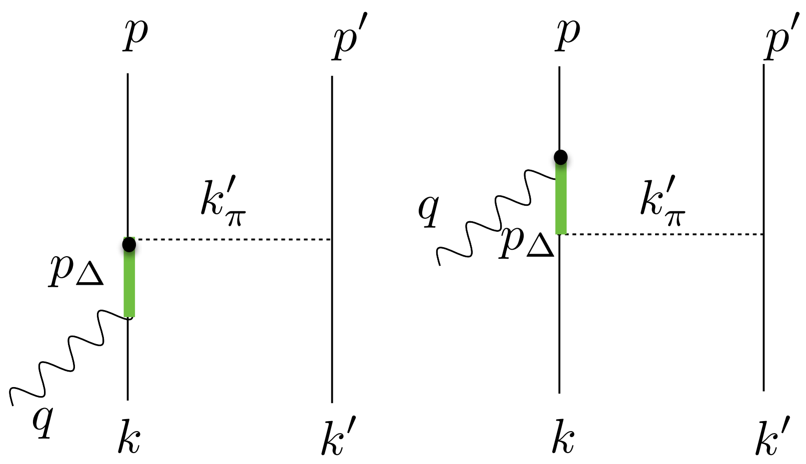

The normalization of the dominant $N \to \Delta$ transition form factor needs be known to 3% precision to achieve 1% cross-section precision for MiniBooNE kinematics

State-of-the-art determinations of this form factor from experimental data on pion electroproduction achieve 10-15% precision (under some assumptions)

Hernandez et al, PRD 81 (2010)

Further constraints on $N \to \Delta$ transition relevant for two-body currents and π production will be necessary to achieve few-percent cross-section precision

ACHILLES: A CHicago Land Lepton Event Simulator

The propagation of **nucleons** through the **<u>nuclear medium</u>** is crucial in the analysis of electron-nucleus scattering and neutrino oscillation experiments.

- Elastic scattering
- Charge exchange
- Pion Production
- Absorption
- ….

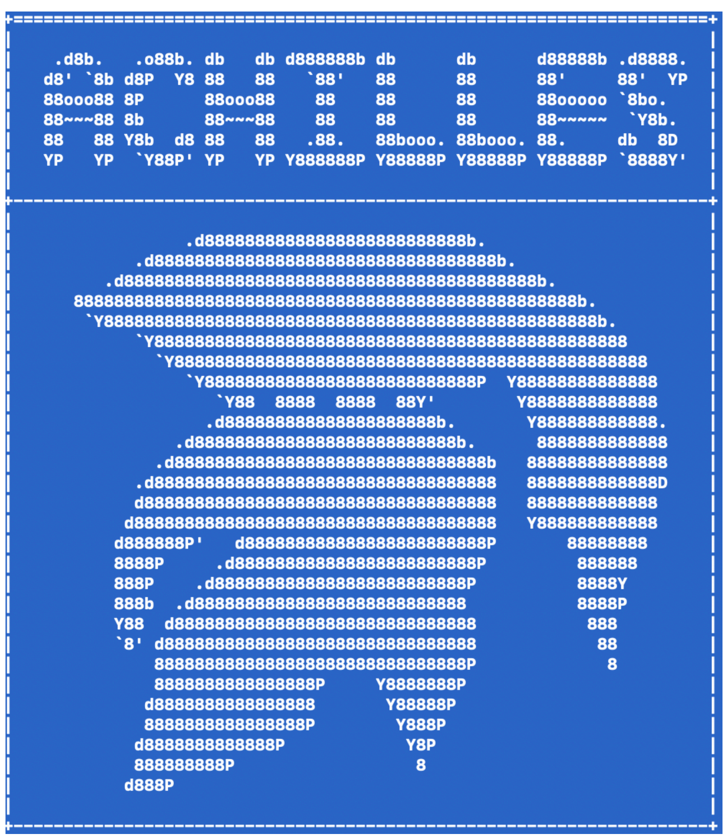

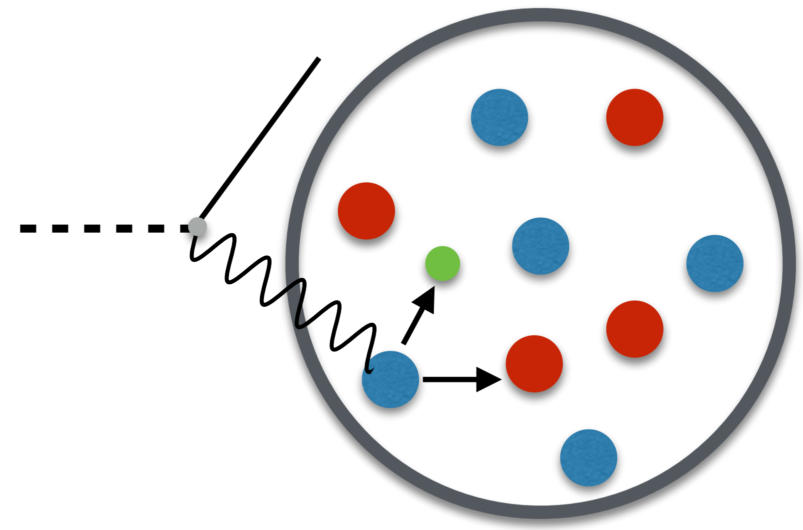

- Develop a theory driven, modular event generator
- Provide automated BSM calculations for neutrino experiments
- Uses realistic QMC nuclear calculations as inputs

J.Isaacson, W Jay, A. Lovato, P Machado, NR:

- *arXiv:2205.06378*
- *PRD 105 (2022) 9, 096006*
- *PRC 103 (2021) 1, 015502*

Fermilab

Noemi Rocco, nrocco@fnal.gov

Algorithm Overview

$$|\mathcal{M}(\{k\} \to \{p\})|^2 \simeq \sum\!\!\!\!\!\!\int_{p'} |\mathcal{V}(\{k\} \to \{p'\})|^2 \times |\mathcal{P}(\{p'\} \to \{p\})|^2$$

- Primary Interaction
- Evolution out of the nucleus (intra-nuclear) cascade

Approximate as incoherent product of primary interaction and cascade

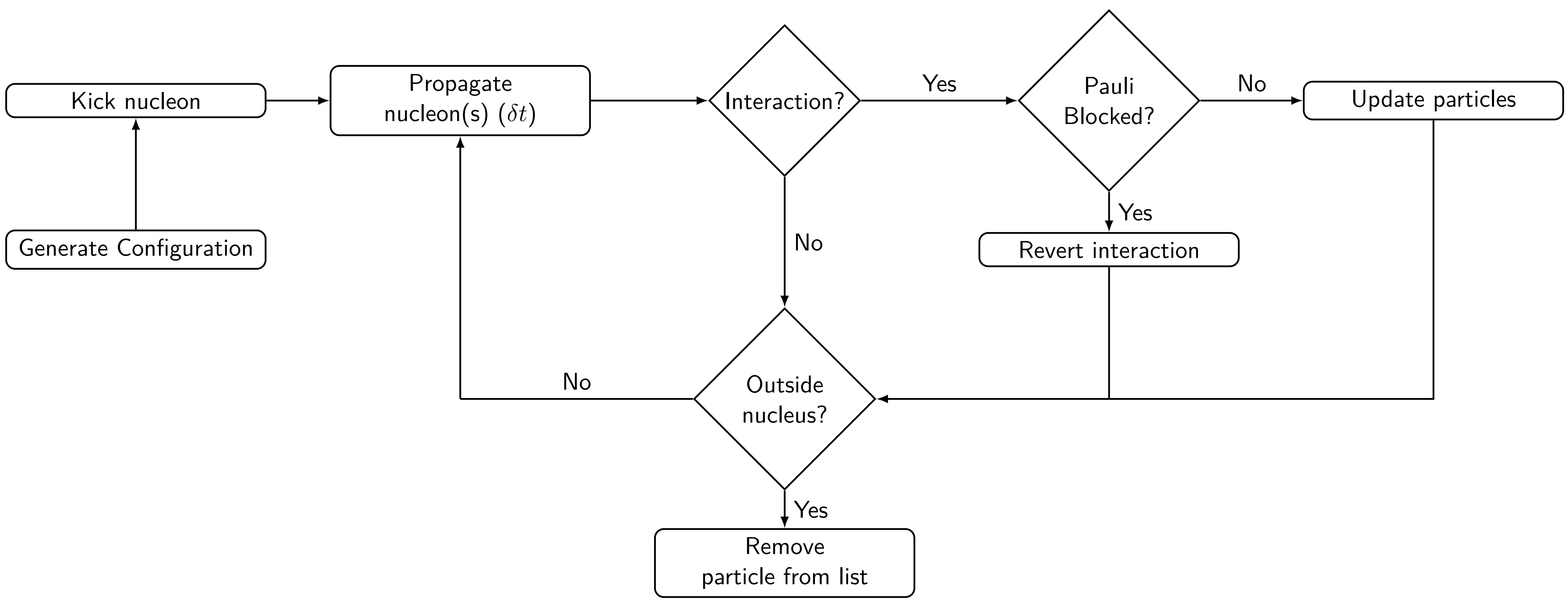

Noemi Rocco, nrocco@fnal.gov

Sampling nucleon configurations

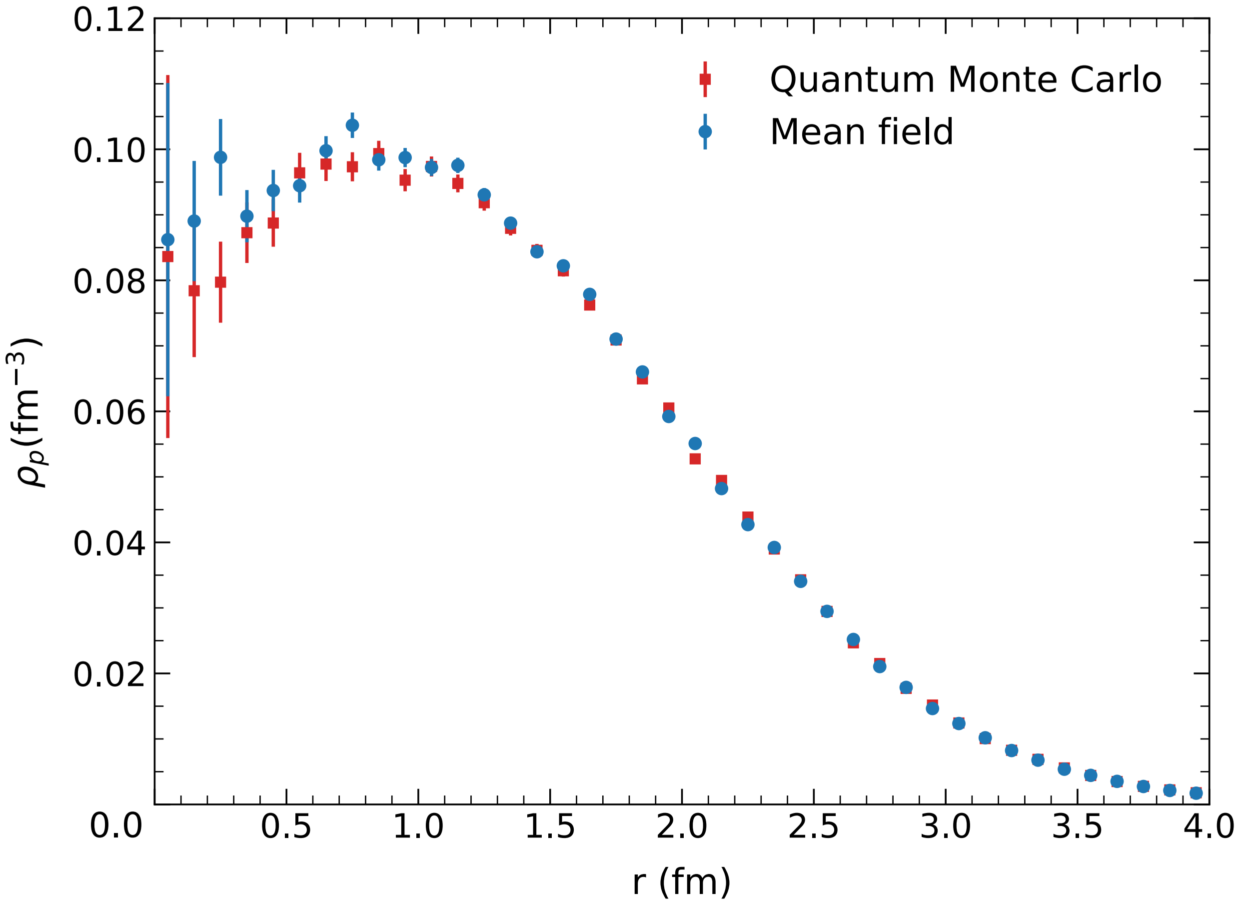

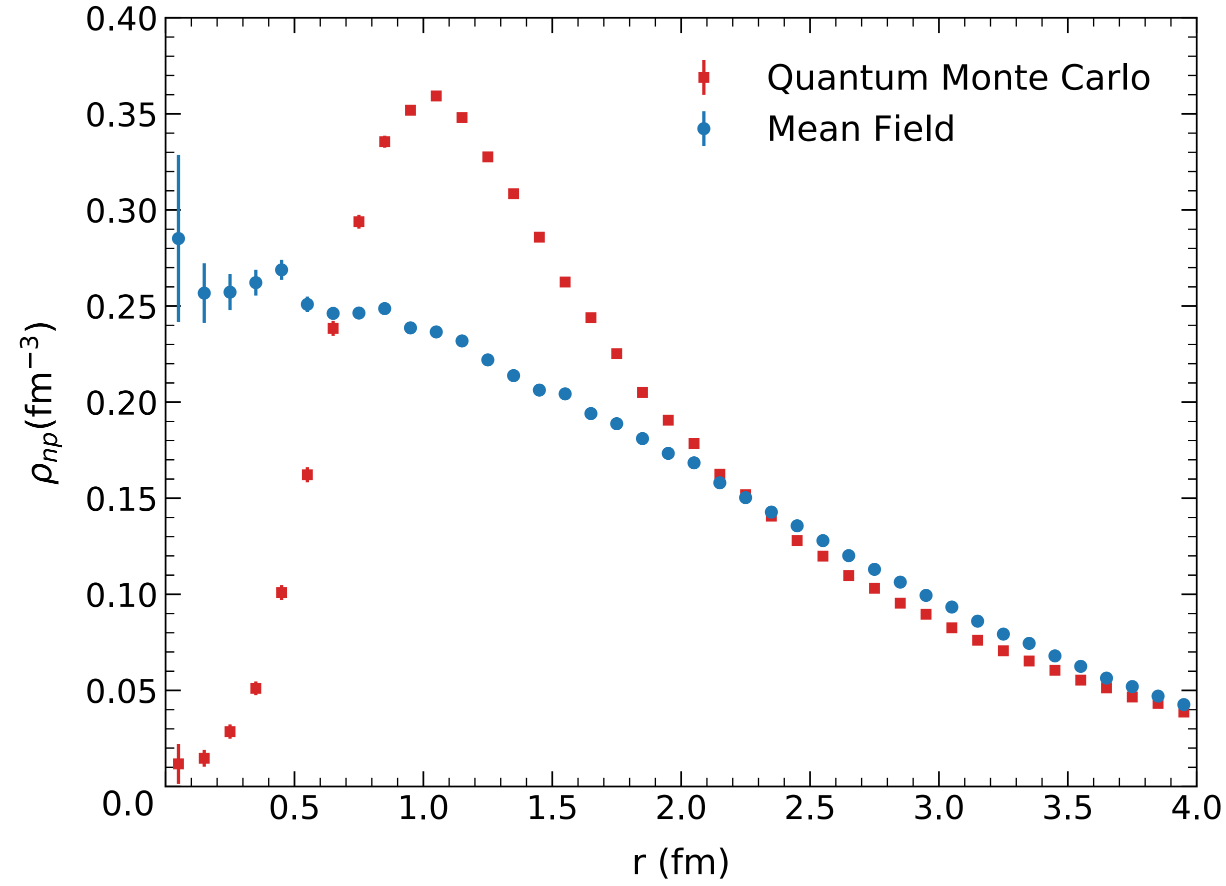

The nucleons' positions utilized in the INC are sampled from **36000 GFMC configurations**. For benchmark purposes we also sampled **36000 mean-field (MF) configurations** from the single-proton distribution.

The differences between GFMC and MF configurations are apparent when comparing the **two-body density distributions**: repulsive nature of two-body interactions reduced the probability of finding two particles close to each other

Noemi Rocco, nrocco@fnal.gov

Fermilab

Probability of interaction

To check if an interaction between nucleons occurs an **accept-reject** test is performed on the **closest nucleon** according to a probability distribution.

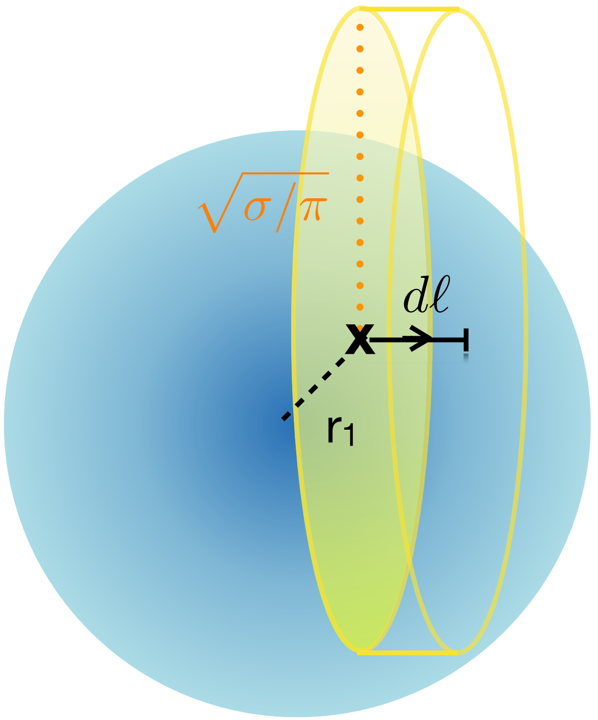

We use a **cylinder probability distribution**, this mimics a more classical billiard ball like system where each billiard ball has a radius

For benchmark purposes, we also implemented the **mean free path approach**, used in some event generators

$$P = \sigma \bar{\rho} d\ell$$

where a constant density is assumed $\rho(r_1) \sim \rho(r_1 + d\ell) \sim \bar{\rho}$

we sample a number $0 \leq x \leq 1$

$$\begin{cases} x < P & \text{the interaction occurred, check Pauli blocking} \\ x > P & \text{the interaction DID NOT occur} \end{cases}$$

Noemi Rocco, nrocco@fnal.gov

Fermilab

Results: p-^{12}C cross section- transparency

Reproducing proton-nucleus cross section measurements is an important test of the accuracy of the INC model.

- The Monte Carlo cross section is defined as:

$$\sigma_{\mathrm{MC}} = A\frac{N_{\mathrm{scat}}}{N_{\mathrm{tot}}}$$

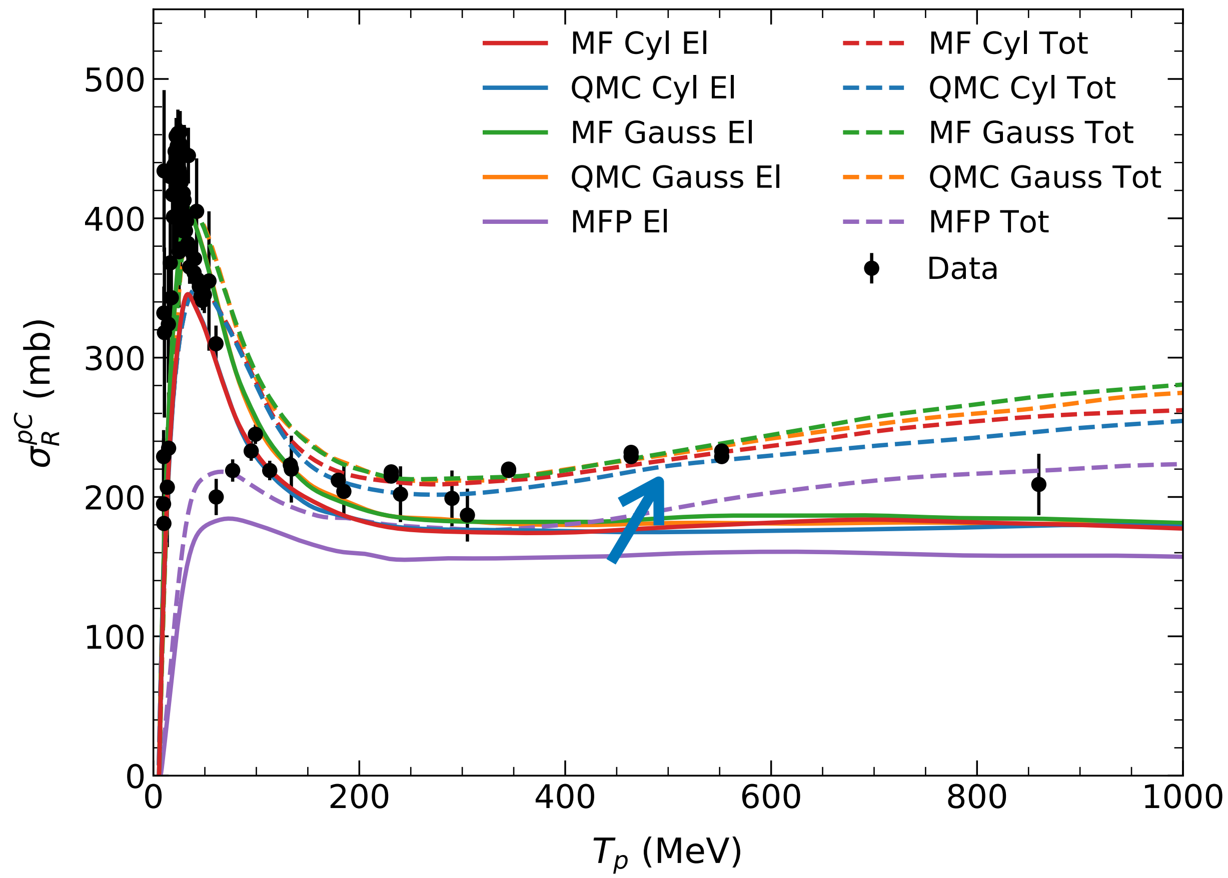

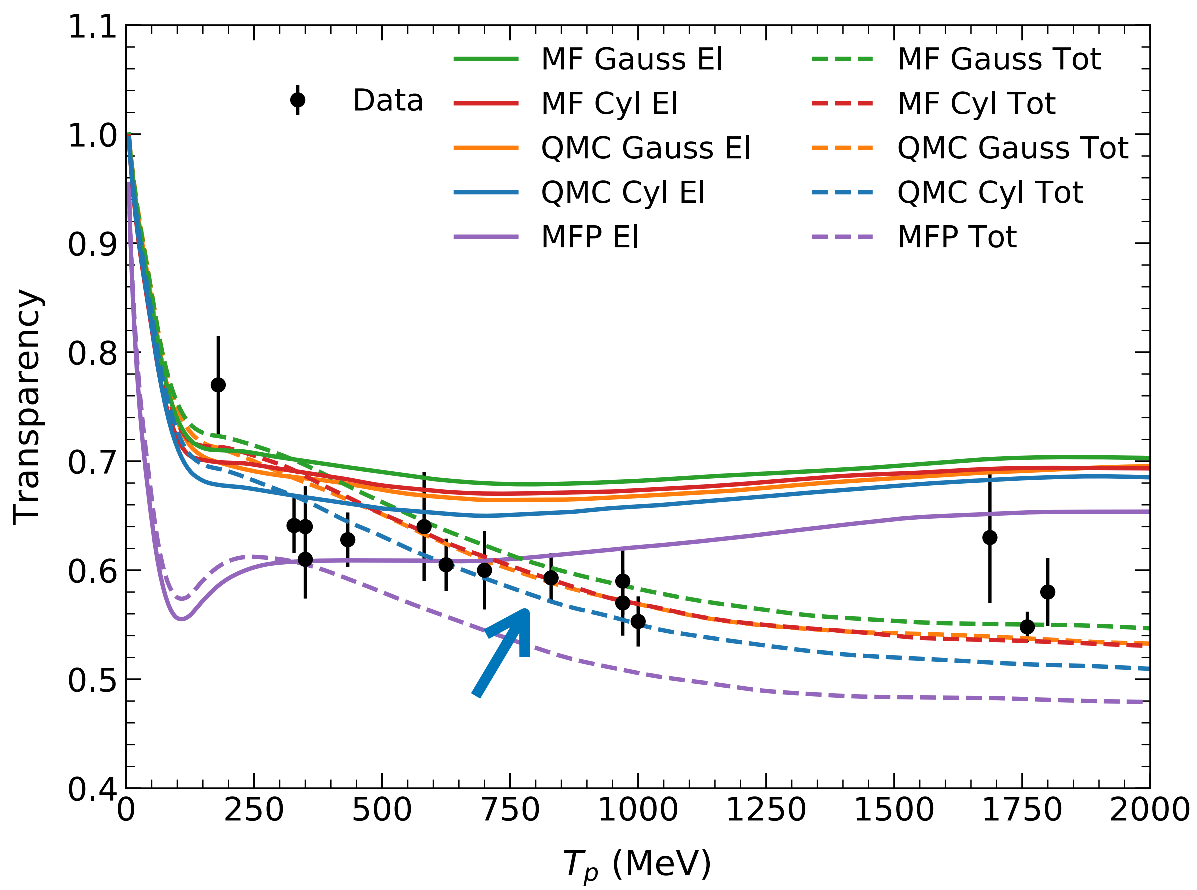

Nuclear transparency is **measured in (e,e'p) scattering** experiments

Simulation: we randomly sample a nucleon with Tp and propagate it through the nuclear medium

$$T_{\mathrm{MC}} = 1 - \frac{N_{\mathrm{hits}}}{N_{\mathrm{tot}}}$$

Noemi Rocco, nrocco@fnal.gov

Inclusion of the Real Optical Potential

The presence of a **mean-field nuclear potential** may trap struck nucleons or deflect their trajectory, effectively changing the number, momentum and direction of outgoing particles.

We introduced two different background potentials, depending on ***r*** and ***p***

- Wiringa, Fiks, Fabrocini, PRC 38, 1010 (1988): $$U(p',r) = \alpha[\rho(r)] + \frac{\beta[\rho(r)]}{1 + (p'/\Lambda[\rho(r)])^2},$$

- Effective Optical Potential — (fitting done using Schroedinger equation) Cooper et al PRC 80, 034605 (2009)

The mean-field nuclear potential enters in two different places:

$$m^*(p',\rho) = p'\left(\frac{p'}{m} + \frac{dU(p',\rho)}{dp'}\right)^{-1}.$$

$$\frac{d\sigma'}{d\Omega} = \frac{|\mathbf{p}'_1 - \mathbf{p}'_2|}{m}\left|\frac{\mathbf{p}'_1}{m^*(p'_1,\rho)} - \frac{\mathbf{p}'_2}{m^*(p'_2,\rho)}\right|^{-1} \times \frac{m^*\left(\sqrt{(p'^2_3 + p'^2_4)/2},\rho\right)}{m}\frac{d\sigma}{d\Omega},$$

- Symplectic integrator to solve the equation of motion of the particle, curved trajectories

Noemi Rocco, nrocco@fnal.gov

CLAS/e4ν collaboration

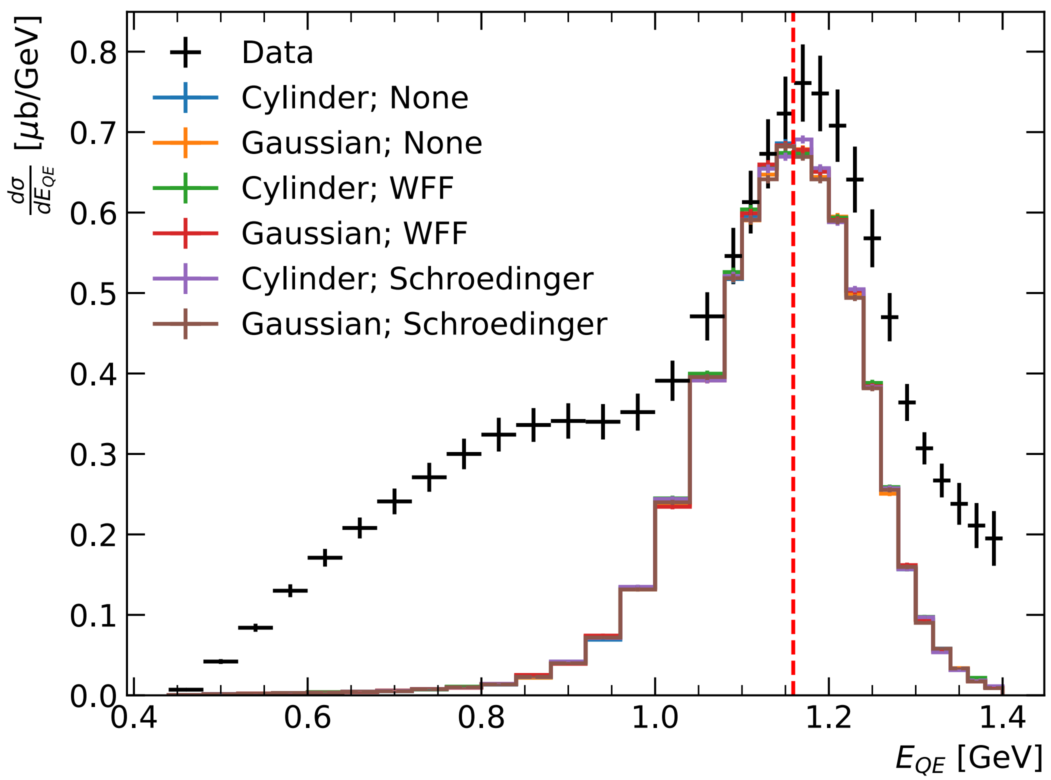

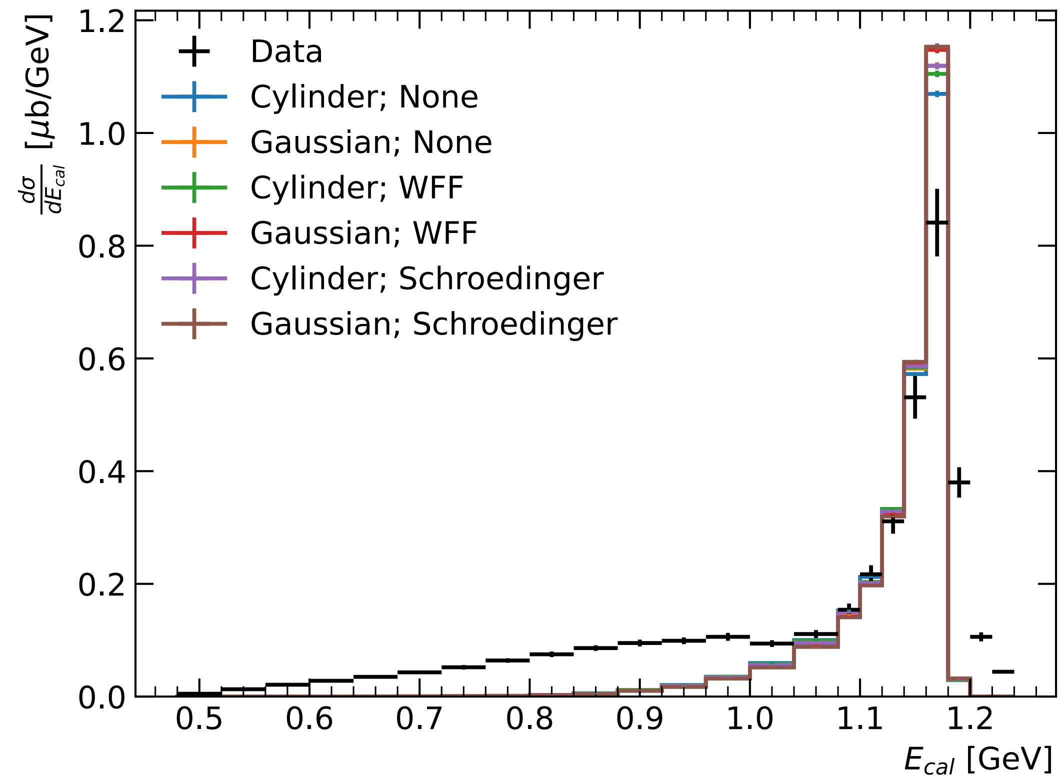

$$\mathrm{E}_{QE} = \frac{2\mathrm{M}\epsilon + 2\mathrm{ME}_l - \mathrm{m}_l^2}{2\left(\mathrm{M} - \mathrm{E}_l + |\mathrm{k}_l|\cos\theta_l\right)}$$

- Mimics energy reconstruction techniques used in Cherenkov detectors

$$E_{\mathrm{cal}} = \sum_i (E_i + \epsilon_i)$$

- Mimics energy reconstruction techniques used in LArTPC detectors: ionization energy

Noemi Rocco, nrocco@fnal.gov

Proposed Measurements

- Exclusive observables that are sensitive to final state interactions: *proton multiplicity energy spectrum*

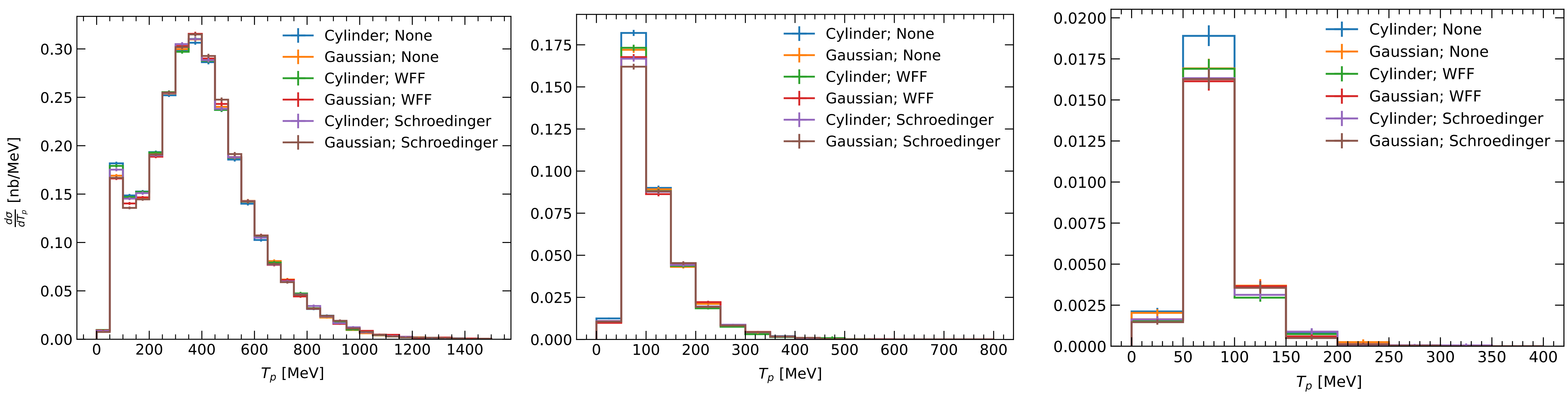

- We consider the 2.257- GeV electron beam, for every event, we count the number of protons that pass experimental cuts
- We take all leading-energy protons in events with at least one proton and build their energy spectrum. Apply the same procedure for all second and third leading protons
- This observable is sensitive to INC and also other reaction mechanisms

Noemi Rocco, nrocco@fnal.gov

Conclusions

GFMC and QMC SF are microscopic approaches able to accurately describe neutrino cross sections

Different sources of uncertainties can be considered:

Nuclear Hamiltonians: different efforts in place to provide UQ in chiral EFT

Form factors: one- and two-body currents.

Error of factorizing the hard interaction vertex / using a non relativistic approach

LQCD will be crucial in providing inputs for form factors and π-production amplitudes

These errors need to be consistently propagated / combined through the intra-nuclear cascade

Achilles is a theory driven, modular event generator. Provides automated BSM calculations for neutrino experiments. Work is currently underway to incorporate pion degrees of freedom

Noemi Rocco, nrocco@fnal.gov

Thank you for your attention!